Current Research (2025) Newfoundland and Labrador Department of Industry, Energy and Technology Geological Survey, Report 25-1, pages 1-38

OROGENIC GOLD MINERALIZATION IN SOUTHERN AND CENTRAL NEWFOUNDLAND: PETROGRAPHIC, FLUID INCLUSION AND SULPHUR ISOTOPE STUDIES

J. Conliffe, H.A.I. Sandeman, I.W. Honsberger[1] and C. Laflamme[2]
Mineral Deposits Section
[1]Natural Resources Canada, Geological Survey of Canada, 601 Booth Street, Ottawa, ON, K1A 0E8
[2]Département de géologie et de génie géologique, Université Laval, Québec

ABSTRACT

*Newfoundland is an emerging gold district containing numerous gold occurrences, including past-producers, known deposits with resource estimates as well as a number of advanced exploration projects. There are strong structural controls on the location of gold occurrences, with most located in second- and third-order fault zones associated with major Paleozoic crustal-scale systems. Mineralization is typically hosted in quartz–carbonate veins, but petrographic and SEM-MLA analyses of mineralized quartz veins highlight significant intra-deposit variability in ore mineralogy and metal associations. Some deposits are associated with abundant base-metal mineralization (*e.g.*, Cape Ray), some with abundant Sb-rich sulphosalts (*e.g.*, Moosehead) and in others, pyrite is the only significant sulphide associated with gold mineralization (*e.g.*, Valentine Lake).*

Fluid-inclusion studies show that mineralizing fluids are low-salinity aqueous-carbonic fluids, with minimum trapping temperatures of ~250–350°C. Isochore modelling show that these fluids were trapped at a wide range of pressures, corresponding to paleodepths of mineralization ranging from deep mesozonal (>10 km) to shallow epizonal (<6 km). In-situ *sulphur isotope analyses of pyrite associated with gold mineralization show both inter- and intra-deposit variability; reflecting variations in sulphur source between deposits (metamorphic* vs. *magmatic–hydrothermal fluid inputs) as well as physiochemical changes in mineralizing fluids during gold deposition.*

The gold occurrences are classified as the crustal-scale fault-associated subtype of Phanerozoic orogenic gold deposits. They formed in multiple cycles during the late stages of the Salinic orogeny and span the Acadian and Neoacadian orogenic cycles, where mineralizing fluids in most occurrences were likely generated via *metamorphic devolatilization during regional metamorphism. However, the sulphur isotope evidence, coupled with the close spatial and temporal association of gold mineralization with voluminous granitoid magmatism, suggests that magmatic–hydrothermal processes may be locally important.*

INTRODUCTION

Newfoundland is host to a large number of gold occurrences associated with Paleozoic crustal-scale fault systems (Honsberger *et al.*, 2019a; 2022a; Sandeman *et al.*, 2022), with more than 500 gold occurrences documented (Newfoundland and Labrador Mineral Occurrence Database (MODS); https://gis.geosurv.gov.nl.ca/mods/mods.asp). These include gold deposits such as Valentine Lake (3.96 Moz Au measured and indicated resource), Cape Ray (0.61 Moz Au indicated and inferred resource), Glover Island (0.18 Moz Au indicated and inferred resource) and Appleton Fault Zone deposits (2.00 Moz Au indicated and inferred resource), as well as a number of other advanced exploration projects. Despite the increased exploration activities in recent years, published geological studies on orogenic gold deposits in Newfoundland are limited compared to major producing gold belts (*see* Sandeman *et al.*, 2022 and references therein).

Orogenic gold deposits in metamorphosed orogenic belts are a major global source of gold production (Frimmel, 2008). These deposits are generally thought to have formed as a result of crustal metamorphic processes during orogenesis (Goldfarb *et al.*, 2005; Dubé and Gosselin, 2007; Goldfarb and Pitcairn, 2023), with mineralizing fluids sourced *via* devolatilization reactions during greenschist-facies metamorphism (Phillips and Powell, 2010) and gold locally sourced from the surrounding metasedimentary or metavolcanic rocks (Pitcairn *et al.*, 2006, 2015). A magmat-

ic component of mineralizing fluids has been proposed for some deposits (*e.g.*, Hammond *et al.*, 2011; Treloar *et al.*, 2015; Spence-Jones *et al.*, 2018; Palinkaš *et al.*, 2024), although the relative importance of magmatic fluids in orogenic gold deposits remains controversial (Goldfarb and Pitcairn, 2023). Orogenic deposits form at a wide range of crustal depths, from epizonal deposits at shallow crustal depths (<6 km), mesozonal deposits formed between 6 and 12 km, to hypozonal deposits that form at depths greater than 12 km, and have a wide range of metal associations but are typically base-metal poor (Groves *et al.*, 1998; Goldfarb *et al.*, 2005). Recent work has shown that rather than representing a single mineral deposit type, orogenic gold deposits, and specifically Phanerozoic orogenic gold deposits, may represent a number of discrete but related mineral deposit types (Mortensen *et al.*, 2022).

Many gold occurrences in Newfoundland have characteristics typical of orogenic gold deposits (Groves *et al.*, 1998, 2003; Goldfarb *et al.*, 2005; Dubé and Gosselin, 2007). These include regional settings in an accretionary orogen with mineralization formed during the syn- to post-collisional phase of orogenesis, spatial association with deep-crustal fault zones that have complex structural histories (mineralization in second or third order fault structures), mineralization hosted in quartz–carbonate veins or disseminated in the wallrock surrounding vein systems, and localization of deposits along deformation corridors within low-grade (sub-greenschist to greenschist facies) terranes adjacent to exhumed, higher grade metamorphic terranes (Evans, 1996, 1999; Dubé and Lauzière, 1997; Conliffe, 2021; Honsberger *et al.*, 2022a, b; Sandeman *et al.*, 2022). Previous studies have identified significant variations in mineralization styles and settings between individual gold occurrences in Newfoundland, including host lithologies, inferred mineralization depths (epizonal to mesozonal) and metal contents (Wilton and Strong, 1986; Evans and Wilson, 1994; Evans, 1996, 1999; Dubé and Lauzière, 1997; O'Driscoll and Wilton, 2005; Conliffe, 2021; Honsberger *et al.*, 2022a, b; Sandeman *et al.*, 2022 and references therein).

This contribution focusses on six gold zones in south and central Newfoundland: 1) the Cape Ray deposits; 2) the Valentine Lake deposits; 3) the Wilding Lake prospects; 4) the Glover Island deposits; 5) the Moosehead prospect; and 6) gold deposits proximal to the Appleton Fault Zone (Dome, Lotto, Keats and Big Vein) (Figure 1). We present geological descriptions of each gold-mineralized zone, as well as detailed observations on the ore mineralogy and distribution of gold in mineralized veins. This is supplemented by fluid-inclusion analysis of auriferous quartz veins and *in-situ* sulphur isotopic analysis of pyrite grains spatially associated with gold mineralization. These data are used to constrain the mineralized fluids and gold precipitation mechanisms in individual gold occurrences and develop improved metallogenic models for the formation of orogenic gold deposits in central and southern Newfoundland, which can be used in future exploration and be applied to these deposit types globally.

REGIONAL GEOLOGICAL SETTING

Orogenic gold mineralization in southern and central Newfoundland is primarily hosted in rocks of the Dunnage Zone of the Canadian Appalachians (Figure 1; Williams, 1979). Based on contrasting pre-Silurian stratigraphic, paleontological and lithogeochemical constraints, the Dunnage Zone is subdivided, along the Beothuk Lake Line (formerly Red Indian Line; van Staal *et al.*, 2024), into the western peri-Laurentian Notre Dame Subzone and the eastern peri-Gondwanan Exploits Subzone (Williams *et al.*, 1988). The zonal terminology for lithotectonic terranes is used herein to be consistent with the differentiation of rock units as defined by mapping (*e.g.*, Colman-Sadd *et al.*, 1990). However, it is noted that this terminology does not encompass the post-Ordovician geology of south and central Newfoundland, with younger cover rocks and pre- to post-tectonic intrusions now correlated across these terrane boundaries and major crustal structures recording a complex history of movement extending from the Ordovician to the Carboniferous.

The Notre Dame Subzone consists of a series of continental and oceanic arcs, back-arc basins and ophiolites, which developed outboard of the Laurentian margin following the opening of Iapetus (van Staal *et al.*, 2007). These were developed on, or thrust over, the hyperextended peri-Laurentian crust of what is now termed the Dashwoods terrane (Waldron and van Staal, 2001; van Staal *et al.*, 2007; van Staal and Dewey, 2023). In the northern part of the Dashwoods terrane, the Lushs Bight Oceanic Tract was obducted over the Dashwoods terrane in the Late Cambrian (500–493 Ma) during the first stage of the Taconic orogeny (van Staal *et al.*, 2007). A series of ophiolite complexes and associated cover rocks, including the Baie Verte Oceanic Tract, Grand Lake Ophiolite Complex and Annieopsquotch Accretionary Tract, developed in marginal basins both inboard and outboard of the Dashwoods terrane during the Ordovician (van Staal *et al.*, 2007). All units were subsequently intruded by magmatic rocks of the Notre Dame Arc, which is interpreted to represent the products of a prolonged continental-arc system (*ca.* 488 to 450 Ma) developed on the trailing edge of the Dashwoods terrane and associated with the closure of the Taconic Seaway and subsequent collisional events during the protracted Taconic orogeny (Whalen *et al.*, 2006; van Staal *et al.*, 2007). These older sequences are unconformably overlain by the *ca.* 435 Ma Springdale volcanic sequence and widely intruded by a variety of gabbroic, granitic and syenitic rocks of comparable Middle to Late

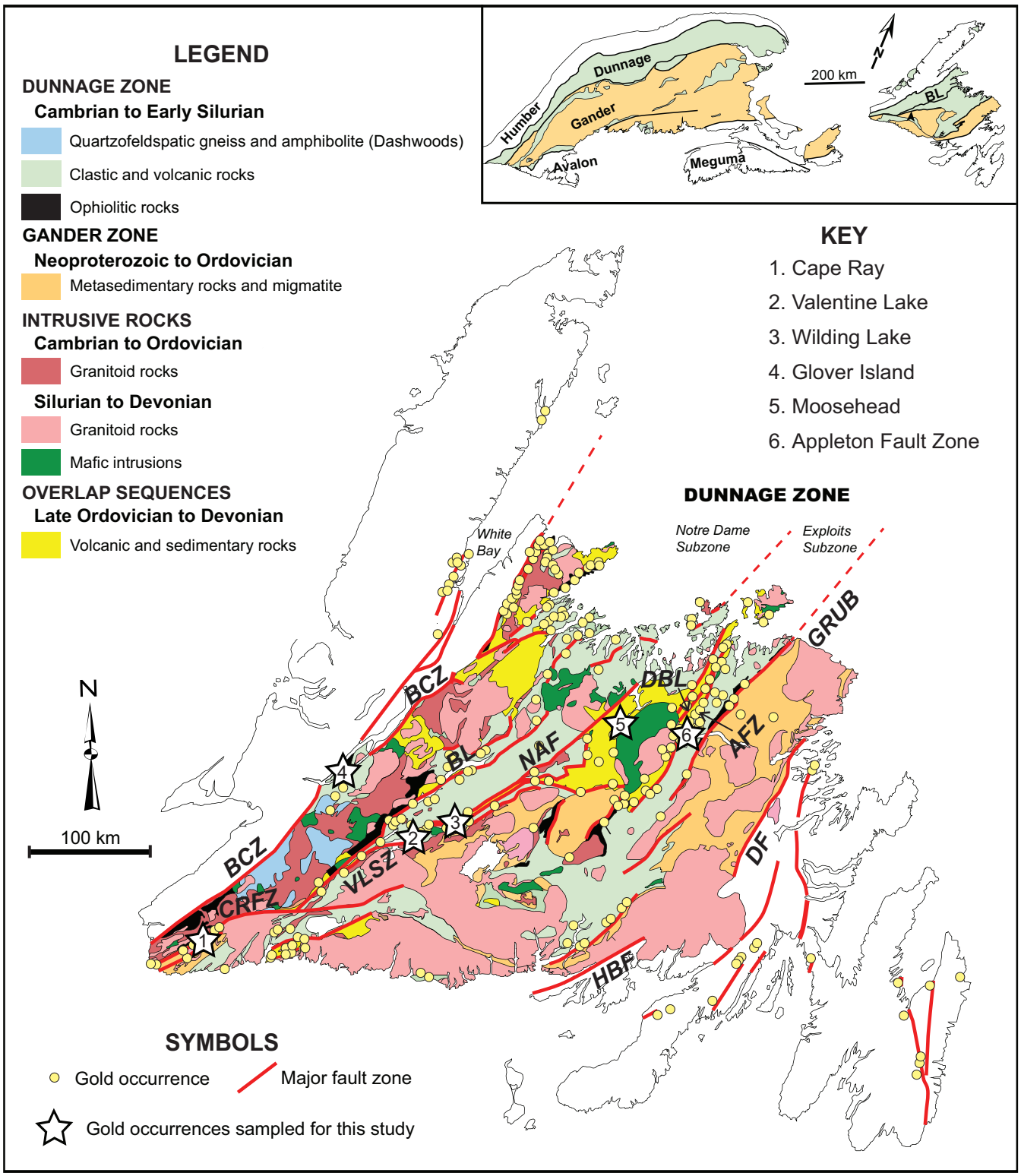

Figure 1. *Simplified geological map of central Newfoundland (Dunnage and Gander lithotectonic zones), showing location of major crustal structures and gold occurrences included in this study (adapted from Honsberger* et al.*, 2019a). Newfoundland geology map adapted after Colman-Sadd* et al. *(1990), with gold occurrences from MODS database. Abbreviations: AFZ–Appleton Fault Zone; BCZ–Baie Verte Brompton Line–Cabot Fault Zone; BL–Beothuk Lake Line; CRFZ–Cape Ray Fault Zone; DBL–Dog Bay Line; DF–Dover Fault; GRUB–Gander River Complex Fault Zone; HBF–Hermitage Bay Fault; NAF–Northern Arm Fault; VLSZ–Valentine Lake Shear Zone.*

Silurian age (Chandler *et al.*, 1987; Coyle and Strong, 1987; Whalen *et al.*, 1997, 2006). In southern Newfoundland, magmatic rocks of the Notre Dame Arc are unconformably overlain by Late Ordovician to Silurian intracontinental volcanic and sedimentary rocks of the Windsor Point Group (Dubé *et al.*, 1996).

The Exploits Subzone of the Dunnage Zone, lying southeast of the Beothuk Lake Line, comprises peri-Gondwanan Neoproterozoic to Ordovician volcanic, sedimentary and plutonic rocks interpreted to have formed in a sequence of arc- to back-arc basins on the leading edge of Ganderia (van Staal and Barr, 2012). The Penobscot and Popelogan–Victoria arc systems represent two distinct phases of subduction along the Gander margin at 515–485 Ma and 475–455 Ma, respectively, separated by the short-lived Penobscot orogeny which thrust these arc- to back-arc systems over Ganderian basement (Neuman, 1967; van Staal and Barr, 2012). These arcs were built on Neoproterozoic basement rocks (*e.g.*, Crippleback and Valentine Lake intrusive suites; Evans *et al.*, 1990; Rogers *et al.*, 2006; Honsberger *et al.*, 2022a). In central Newfoundland, arc complexes of the Exploits Subzone are conformably overlain by Late Ordovician to Silurian turbiditic shales and sandstones of the Badger Group, which record evidence of Laurentian derived detritus (Waldron *et al.*, 2012) on rocks of Ganderia and thus mark the stitching of the Notre Dame and Exploits subzones along the Beothuk Lake Line during the terminal Taconic orogeny. These turbidites, in turn, are overlain by Late Silurian to Early Devonian volcano-sedimentary rocks, including the Botwood and Indian Islands groups in central Newfoundland (Honsberger *et al.*, 2022a, b) and the La Poile Group in southern Newfoundland (O'Brien *et al.*, 1991). Honsberger *et al.* (2022a) suggested that the formation of these Silurian basins and associated magmatism between *ca.* 427 and 418 Ma represented an episode of extension associated with asthenospheric and crustal magmatism related to slab break-off during the transition from the late Salinic (*ca.* 435 Ma) to early Acadian (*ca.* 418 Ma) orogenic cycles.

The Notre Dame and Exploits subzones are bounded and cut by a number of crustal-scale faults and structural corridors, which form the loci for significant orogenic gold mineralization (Figure 1). Some of the major fault zones associated with gold mineralization discussed in this article include the Baie Verte Brompton Line–Cabot Fault Zone, Cape Ray Fault Zone, Valentine Lake Shear Zone, Victoria Lake Shear Zone and Appleton Fault Zone (Figure 1; Evans, 1996; Dubé *et al.*, 1996; Dubé and Lauzière, 1997; Brem, 2007; Waldron *et al.*, 2015; Conliffe, 2021; Honsberger *et al.*, 2022a, b, 2023; Sandeman *et al.*, 2022). These crustal-scale structures in central Newfoundland record a complex, commonly protracted, history of compression, extension and strike–slip movement during multiple orogenic events extending from the Ordovician to the Carboniferous (Waldron *et al.*, 2015; Kellett *et al.*, 2016).

METHODOLOGY

SAMPLING AND PETROGRAPHY

Representative samples of mineralized quartz veins were collected during fieldwork between 2018 and 2024. In total, 32 samples with abundant sulphides and sulphosalts associated with gold mineralization were analyzed from the six study areas. Sample details are summarized in Table 1.

Petrographic analysis of polished thin sections was conducted in transmitted and reflected light on an Olympus BX1 microscope at the Geological Survey of Newfoundland and Labrador. Following initial screening, fourteen samples were analyzed using a FEI MLA 650FEG scanning electron microscope (SEM) at the Memorial University of Newfoundland Micro Analysis Facility (MUN MAFIIC). Qualitative analyses were completed using high throughput Energy-dispersive X-ray Spectroscopy (EDX) detectors from Bruker (https://www.mun.ca/creait/). Panchromatic cathodoluminescence (CL) imaging was undertaken on four samples using the JEOL JSM 7100 F SEM at Memorial University equipped with a Deben Centaurus CL detector, under an accelerating voltage of 15kV and working distance of 13 mm. Eight samples were also selected for optical cathodoluminescence (CL) imaging at the Paleoenvironment and Diagenesis Research Group at Memorial University of Newfoundland. CL imaging was conducted using a CITL Mk5 cold cathodoluminescence system (operating conditions 10–15 kV and 250 μA) attached to a Zeiss Axio Scope A1 HAL 50. For samples 21HVB-412B, 21HVB-412C and 21HVB-421D, energy dispersive spectroscopy (EDS) analyses were performed on polished thin sections at the Geological Survey of Canada, Ottawa, ON using a Zeiss EVO50 SEM equipped with an EDS system from Oxford Instruments consisting of a X-Max 150 silicon drift detector and AZtec acquisition software. Analyses for these samples were performed using an accelerating voltage of 20 kV, working distance of 8.5 mm, probe current of 1 nA, and acquisition time of 3 s.

FLUID-INCLUSION PETROGRAPHY AND MICROTHERMOMETRY

Petrographic descriptions of fluid inclusions were carried out using the fluid inclusion assemblage (FIA) method (Goldstein and Reynolds, 1994) and Goldstein (2003). Care was taken to select samples with representative FIAs in gangue quartz associated with gold and sulphide mineralization and without evidence of post-entrapment modification

Table 1. Sample locations, gold grades and analyses conducted during this study. Gold assay data from Cape Ray, Wilding Lake, Glover Island and Appleton Fault Zone were obtained from GSNL samples analyzed by Instrumental Neutron Activation Analysis (INAA). Assay data from Valentine Lake and Moosehead were taken from >1 m intervals encompassing sample location, with analysis by Fire Assay-Atomic Absorption (FA-AA). All coordinates in UTM Zone 21, datum NAD27.

Sample	Area	Prospect	Sample type	Easting	Northing	Drillhole	Depth (m)	Au grade (ppb)	Analysis Type			
									SEM-MLA	CL Imaging	Fluid Inclusion	Sulphur Isotopes
HS19-071	Cape Ray	41 Zone	Stockpile	355860	5291040			9470	x		x	
HS19-070C		51 Zone	Outcrop	355491	5290719			8710	x		x	
HS19-070D			Outcrop	355491	5290719			11800				x
HS19-070E			Outcrop	355491	5290719			5750		x	x	x
HS19-072C		Windowglass Hill	Outcrop	352910	5289305			1750	x			
HS19-072D			Subcrop	352910	5289305			70900		x	x	x
21JC-C405	Valentine Lake	Berry	Drillcore	490412	5358442	VL-21-1066	70.25 to 70.43	595		x	x	x
21JC-C401		Leprechaun	Drillcore	486775	5355843	VL-19-722	21.5 to 22.63	886			x	
21JC-C411			Drillcore	486425	5355619	VL-17-654	258.85 to 259.08	2995		x		x
21JC-C412			Drillcore	486425	5355619	VL-17-654	106.6 to 106.73	1168			x	
21JC-C409		Marathon	Drillcore	492681	5360355	MA-17-245	281.84 to 281.92	566			x	
21JC-C410			Drillcore	492681	5360355	MA-17-245	397.38 to 397.55	3546			x	x
HS18-129A	Wilding Lake	Alder	Outcrop	517265	5367733			4910				
HS18-129B			Outcrop	517265	5367733			954				
HS18-115		Elm Zone	Outcrop	518372	5368026			13200	x	x	x	
HS18-130B			Outcrop	518277	5367995			25500			x	
HS18-130E			Outcrop	518277	5367995			20100	x	x		
19JC-C030	Glover Island	Kettle Pond South	Drillcore	441894	5395385	KPS-2	57.4 to 57.58	44200	x			
19JC085A01		Lunch Pond	Outcrop	441997	5394595			29200	x			
19JC-C005		Lunch Pond South East	Drillcore	441700	5394650	LPSE-1	71.4 to 71.63	19500	x			x
19JC-C111			Drillcore	441358	5394244	LPSE-11-57	350.05 to 350.23	6520		x		x
23JC-202	Moosehead	Eastern Trend	Drillcore	613668	5428358	MH-22-505	202.18 to 202.38	28486		x		x
23JC-203			Drillcore	613668	5428358	MH-22-505	206 to 206.16	5037	x			
HS-19-66_1			Drillcore	613846	5428259	MH-19-62	241.5 to 241.6	55349				x
HS-19-66_2			Drillcore	613846	5428259	MH-19-62	241.5 to 241.6	55349	x			
21HVB-421D	Appleton	Dome	Outcrop	658707	5428733			2300	x			
Dome 1	Fault Zone		Outcrop	658650	5428550			1260	x			
21HVB-412B		Keats	Outcrop	657917	5427273			3400	x			
21HVB-412C			Outcrop	657917	5427273			730		x		x
Big Vein 2		Kingsway	Outcrop	661589	5435225			138		x	x	
Lotto Vein 1		Lotto	Outcrop	658760	5428920			761	x	x	x	
Lotto Vein 2			Outcrop	658760	5428920			89		x		

(*e.g.*, necking, leaking, decrepitation). Therefore, fluid inclusions were only studied in samples with primary FIAs along growth zones, or FIAs of indeterminate origin in clear quartz associated with sulphide and gold mineralization, and without evidence of post entrapment modification (13 of the 32 samples).

Following initial screening of samples to record the presence of suitable FIAs, double polished fluid inclusion wafers (~100 μm thick) were prepared from representative mineralized samples. Microthermometric fluid-inclusion analyses at Memorial University of Newfoundland used a Linkam THMSG600 heating–freezing stage mounted on an Olympus BX51 microscope, with results summarized in Table 2. The analytical data will be released in an upcoming time-release open file. The heating–freezing stage was calibrated using synthetic H_2O and CO_2-H_2O fluid inclusion standards, with calibration measurements at melting point of CO_2 (-56.6°C), melting point of H_2O (0.0°C) and critical point of H_2O (374.1°C). Samples were cooled to -160°C and subsequently heated and the following phase measurements were recorded: melting temperature of carbonic phases (T_m CO_2), last melting temperature of ice (T_m ice), clathrate melting (T_m clath), homogenization temperature of carbonic phases (T_h CO_2) and total homogenization temperature (T_h tot), as well as the mode of homogenization (to liquid, vapour or critical phases). If inclusions decrepitated prior to total homogenization this temperature was also recorded. The volumetric proportion of the carbonic phase was estimated after T_h CO_2 (vol. CO_2/vol. total in percentage). For aqueous-carbonic fluid inclusions these microthermometric measurements were used to calculate the volume fraction of CO_2 (X_{CO2}), fluid salinity (eq. wt. % NaCl), bulk fluid density (in g/cm^3) and isochore slopes using the spreadsheet provided by Steele-MacInnis (2018) for the H_2O-CO_2-NaCl system. In inclusions with low CO_2 contents (generally <0.02 X_{CO2}), salinities were calculated from clathrate melting temperatures using the modelling software packages CLATHRATES and FLUIDS of Bakker (1997, 2003).

SULPHUR ISOTOPES

In situ laser ablation-inductively coupled plasma mass spectrometry (LA-ICPMS) sulphur isotope analysis of pyrite was carried out on 11 samples at the Département de Géologie et Génie Géologique, Université Laval, with full analytical methods outlined in Barre and LaFlamme (2023). Sulphur isotope measurements were completed using an Applied Spectra RESOlution-SE 193 nm ArF excimer laser ablation system coupled to an Agilent 8900 ICP-QQQ-MS. Pyrite was ablated in thin section with a crater diameter of 80 μm, a fluence of 2 J/cm^2, and a repetition rate of 18 Hz. Ablations lasted 30 seconds and aerosol was transported to the ICPMS by 380 mL/min He and 900 mL/min Ar carrier gas. Ablations were followed by 60 s of background to allow sulphur to washout of the cell. The primary reference material for pyrite was Sierra pyrite ($\delta^{34}S$ = 2.2‰ ± 0.18; LaFlamme *et al.*, 2016), and this was used to correct for instrumental fractionation. A secondary reference material used to verify the accuracy of the data was Iberia pyrite ($\delta^{34}S$ = 8.9‰ ± 1.1). Measurements of unknowns are pooled in groups of four, occurring within the same textural domain of the same grain, and uncertainty on each population is estimated as the reproducibility of the primary reference material during the analytical run which approximates ± 1.5‰. Sulphur isotope values in Table 3 represent the average and standard deviation of results from up to 6 individual spots in each pyrite grain. In larger pyrite grains, sulphur isotope data are separate in analyses from the cores and rims.

GEOLOGICAL SETTING AND RESULTS FOR THE GOLD MINERALIZED ZONES

CAPE RAY DEPOSITS

The Cape Ray gold deposits are located in southwestern Newfoundland, close to the Cape Ray Fault Zone (CRFZ; Figure 1), and consist of four known deposits (Central Zone, Windowglass Hill, Isle Aux Mort and Big Pond deposits). These deposits have a combined indicated and inferred resource of 0.61 Moz gold (9.7 Mt at 1.96 g/t Au), with >90% of this resource in the Central Zone and Windowglass Hill deposits (Matador Mining Limited JORC Mineral Resource estimate, May 2023). The local geology consists of Ordovician to Silurian submarine to subaerial volcanic rocks and intracontinental, largely terrestrial sedimentary rocks of the Windsor Point Group, which unconformably overlie Ordovician volcanic-arc rocks of the Dashwoods terrane and are intruded by, and/or associated with, the *ca.* 424 Ma Windowglass Hill Granite (Dubé and Lauzière, 1997). To the southeast, the Windsor Point Group is structurally overlain by deformed gneisses and tectonites of the Early to Middle Ordovician Grand Bay Complex along the steeply southeast-dipping CRFZ, which forms the boundary between the Notre Dame and Exploits subzones and is interpreted as the southern extension of the Victoria Lake Shear Zone and the Beothuk Lake Line in central Newfoundland (Dubé *et al.*, 1996; van Staal *et al.*, 2024). The Windsor Point Group and Grand Bay Complex were subsequently intruded by the Strawberry Granite (384 ± 2 Ma) and Isle aux Morts Granite (386 ± 3 Ma) (Dubé *et al.*, 1996).

The Central Zone Deposit is hosted in strongly deformed graphite–chlorite–sericite schists of the Windsor Point Group close to the tectonic contact with the Grand Bay Complex, and mineralization is associated with a northeast-trending fault that dips moderately to the southeast (Wilton

Table 2. Microthermometric data of quartz-hosted fluid inclusions from gold occurrences in southern and central Newfoundland

Deposit	Sub-deposit	Sample	n	Type		Fill	T_m CO_2 °C	T_m clath °C	T_h CO_2 °C	to	T_h tot °C	to	T decrep °C	X_{CO2}	wt. % NaCl	P@350°C bars	P@500°C bars
Cape Ray	51 Zone	HS19-070C	9	Three phase	Av	0.62	-61.4	5.9	20.2	L	307.6	L	311.0	0.15	7.8	3424	5174
					StDev	0.04	0.4	1.7	0.8		14.3		18.9	0.03	3.1	385	656
			3	Clathrate	Av	0.70		6.1			248.8	L		0.03	9.6		
					StDev	0.00		0.1			2.7			0.00	0.2		
		HS19-070E	4	Three phase	Av	0.55	-59.4	7.1	19.6	L	290.5	V		0.23	5.7	2918	4267
					StDev	0.06	0.1	0.1	0.9		13.9			0.05	0.1	197	383
			6	Carbonic	Av	0.00	-61.6		10.8	L			270.0	1.00			
					StDev	0.00	1.5		10.8				-	-			
			4	Clathrate	Av	0.80		4.9			231.9	L		0.03	11.5		
					StDev	0.00		0.1			14.7			0.00	0.2		
	41 Zone	HS19-071	13	Three phase	Av	0.17	-64.0	7.9	3.7	L	350.0	V	300.0	0.61	4.5	2819	3812
					StDev	0.04	3.4		2.9		29.3		-	-			
			6	Carbonic	Av	0.00	-62.5		1.9	L				1.00			
					StDev	0.00	0.1		5.6					-			
	Windowglass Hill	HS19-072D	5	Three phase	Av	0.60	-58.2	7.1	8.3	L			270.0	0.23	5.6	3638	5138
					StDev	0.06	0.0	0.1	3.8				-	0.02	0.2	105	207
			12	Carbonic	Av	0.00	-60.0		23.2	L				1.00			
					StDev	0.00	2.8		3.1					-			
			1	Clathrate	Av	0.60		7.9			257.8	L		0.03	6.4		
Valentine Lake	Lepreuchaun	21JC-C401	5	Three phase	Av	0.42	-56.6	7.8	27.0	L	279.0	V		0.33	4.3	1716	2597
					StDev	0.07	0.0	0.0	1.1		4.2			0.08	0.0	401	599
		21JC-C412	23	Three phase	Av	0.50	-57.6	7.8	24.1	L	300.8	L, V	245.8	0.24	4.3	2404	3641
					StDev	0.09	0.8	0.4	3.4		11.0		23.5	0.06	0.8	230	391
	Marathon	21JC-C409	12	Three phase	Av	0.55	-57.0	8.3	23.6	L	301.9	V	288.6	0.21	3.4	2610	3945
					StDev	0.04	1.7	0.3	1.1		8.5		12.7	0.02	0.6	67	136
		21JC-C410	23	Three phase	Av	0.61	-58.7	6.1	27.0	L	315.7	V, C	285.0	0.16	7.1	2556	4032
					StDev	0.03	1.4	2.0	2.0		41.9		14.0	0.02	3.2	367	567
	Berry	21JC-C405	15	Three phase	Av	0.45	-57.2	7.6	26.7	L	347.5	V	293.5	0.25	4.6	2069	3186
					StDev	0.15	0.7	0.6	2.9		4.6		28.2	0.12	1.2	561	810
Wilding Lake	Elm	HS18-115B	7	Three phase	Av	0.49	-56.8	8.0	28.6	L	322.3	V	250.0	0.23	4.0	1971	3106
					StDev	0.09	0.3	0.4	0.2		3.1		40.0	0.08	0.8	326	589
		HS18-130B	12	Three phase	Av	0.3	-56.8	8.5	26.8	L	288.3	V	250.0	0.35	3.1	1853	2750
					StDev	0.1	0.1	0.4	2.5		3.0		-	0.08	0.8	361	633
Appleton Fault Zone	Big Vein	BigVein2	12	Three phase	Av	0.69	-58.7	7.5	26.4	V	297.1	L		0.06	4.7	1190	2783
					StDev	0.05	2.1	0.6	1.2		19.9			0.00	1.3	17	573
	Lotto	LottoVein1	11	Three phase	Av	0.75	-57.2	8.4	28.3	V	262.8	L		0.07	3.1	1337	2876
					StDev	0.05	0.1	0.1	0.9		21.6			0.00	0.1	64	75

Table 3. Results of *in-situ* LA-ICP-MS sulphur isotope analysis of pyrite grains from gold occurrences in southern and central Newfoundland

Deposit	Sample	Pyrite grain	$\delta^{34}S$ Average	$\delta^{34}S$ StDev	n
Cape Ray	HS19-070D	1	0.8	2.2	7
		2	1.0	1.1	4
		3	1.0	0.5	5
		Total	0.9	1.5	16
	HS19-070E	1	0.7	5.4	4
		2	1.8	1.9	4
		Total	1.2	3.8	8
	HS19-072D	1	-2.1	1.1	3
		2	4.4	1.6	4
		3	5.1	3.2	4
		4 (core)	3.3	0.9	3
		4 (rim)	5.1	1.7	3
		Total	3.4	3.2	17
Valentine Lake	21JC-C405	1c	7.3	2.3	4
		1r	9.5	1.5	3
		Total	8.2	2.2	7
	21JC-C410	11	10.2	3.4	6
		1 (core)	11.9	1.1	3
		1 (rim)	9.2	1.7	3
		6 (core)	9.4	1.2	3
		6 (rim)	10.1	2.8	3
		Total	10.1	2.4	18
	21JC-C411	1	9.8	2.9	6
		2	10.8	0.0	2
		3	9.5	0.9	3
		Total	9.9	2.1	11
Glover Island	19JC-C005	1 (core)	3.4	1.5	1
		1 (rim)	8.8	0.0	3
		11 (core)	2.9	0.0	1
		11 (rim)	8.3	0.6	3
		6 (core)	6.6	1.7	2
		6 (rim)	10.0	0.9	2
		Total	6.7	2.9	12
	19JC-C111	1	5.1	4.5	4
		3	4.2	1.1	4
		4	5.8	2.8	4
		Total	5.0	2.9	12
Moosehead	23JC-C202	1	8.4	4.0	4
		2	4.7	0.7	3
		4	6.8	3.4	4
		Total	6.8	3.3	11
	HS19_066-1	1	4.4	1.6	4
		Total	4.4	1.6	4
Queensway	21HVC-412C	2	-0.4	2.2	4
		4	-3.2	1.7	4
		Total	-1.8	2.3	8

and Strong, 1986; Dubé and Lauzière, 1997). Several mineralized quartz-breccia veins occur in the fault zone, the most important of which are the A and C veins (Dubé and Lauzière, 1997; Plate 1A). The Windowglass Hill Deposit occurs in the relatively undeformed Windowglass Hill Granite (Dubé and Lauzière, 1997). Mineralization occurs in a series of flat to gently dipping banded veins (Dubé and Lauzière, 1997; Plate 1B). The granitic host rock surrounding the veins is characterized by intense alteration in close proximity to the veins, with disseminated pyrite and moderate to intense sericitization of feldspars (Dubé and Lauzière, 1997). The Cape Ray deposits were formed during the interval *ca.* 418–386 Ma based on crosscutting relationships and muscovite and biotite $^{40}Ar/^{39}Ar$ geochronology of the host rocks (Dubé *et al.*, 1996).

Vein Petrography

Detailed petrographic analysis was conducted on four samples from the Central Zone (three from the 51 Zone and one from the 41 Zone) and two samples from the Windowglass Hill Deposit (Table 1). All samples are mineralized, with gold values of 1.8 to 70.1 g/t Au and significant base-metal mineralization (up to 2.16% Cu, 2.53% Pb and 0.70% Zn).

Mineralized veins in the Central Zone Deposit consist of fragments of deformed host rocks in a matrix of hydrothermal quartz with minor chlorite and muscovite and trace carbonates (calcite and ankerite), apatite, rutile, monazite, xenotime and zircon. Quartz is commonly strongly recrystallized and brecciated, with fragments of early inclusion-rich quartz crosscut by later clear quartz veins (Plate 1C). Sulphides are abundant, locally making up ~40% of the vein but typically comprising between 5 and 10% of the mineralized veins (Wilton and Strong, 1986; Dubé and Lauzière, 1997). Variable proportions of pyrite, chalcopyrite, galena and sphalerite occur as complex intergrowths and cement late brecciation of the quartz veins (Plate 1D). Gold occurs in minute (<100 μm) electrum grains (15.8 to 20.4 wt. % Ag) intergrown with, or as inclusions in sulphides. Late alteration of sulphides to goethite and covellite is also observed (Plate 1D).

In the Windowglass Hill Deposit, mineralized veins consist of quartz-rich and sulphide-rich layers, with evidence for open space filling textures and multiple pulses of sulphide and quartz precipitation (Dubé and Lauzière, 1997). Some sulphide-rich bands contain up to 50% sulphide minerals, with pyrite being the most common phase and chalcopyrite and galena comprising local layering. Quartz in sulphide-rich bands shows evidence of recrystallization and forms a mosaic of fine-grained quartz. Minor sphalerite is also recorded, as well as trace amounts of chlorite, albite, calcite and xenotime. Secondary alteration of sulphide minerals is locally common, with pyrite altered to goethite and chalcopyrite altered to covellite. Gold occurs in electrum grains (31.3 to 46.7 wt. % Ag) intergrown with pyrite and chalcopyrite or forms discrete inclusions in pyrite grains (Plate 1F).

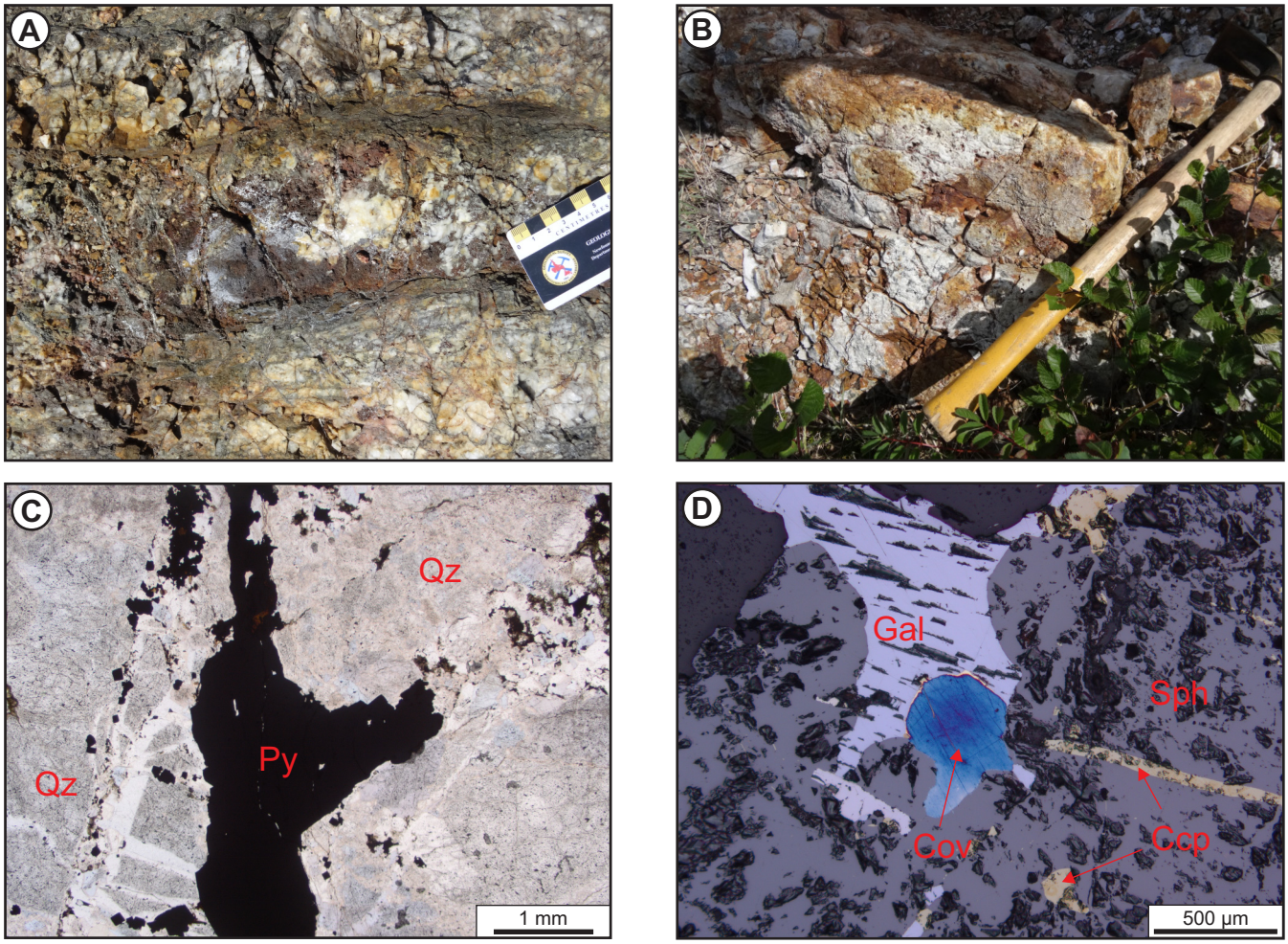

Plate 1. *Representative photographs and photomicrographs from the Cape Ray deposits. A) Brecciated quartz vein with abundant pyrite, galena and chalcopyrite in trench at the 51 Zone, Central Zone Deposit; B) Flat-lying quartz–pyrite–chalcopyrite vein cutting the Windowglass Hill Granite; C) Brecciated and partially recrystallized quartz vein cut by pyrite veinlet (sample HS19-070C, PPL); D) Complex intergrowth of sphalerite, galena and chalcopyrite in mineralized quartz vein, with later supergene covellite (sample HS19-070E, RL).*

Fluid-Inclusion Studies

Fluid-inclusion assemblages suitable for microthermometric analysis were observed in four samples, three from the Central Zone Deposit (41 and 51 zones) and one from the Windowglass Hill Deposit (Table 2). Gangue quartz in all samples is commonly recrystallized or generally cloudy with a high density of fluid inclusions, making determination of fluid inclusion paragenesis difficult. In addition, there is abundant evidence for decrepitation of fluid inclusions post entrapment, with large, decrepitated inclusions surrounded by small neonate inclusions. Primary FIAs and clusters of inclusions of indeterminate origin with no evidence of post-entrapment modification are restricted to clear quartz associated with sulphide minerals (Plate 1G).

Three inclusion types were identified in primary and indeterminate origin FIAs. Aqueous-carbonic inclusions were characterized by the appearance of separate carbonic phases (L_{CO}-V_{CO2}) during freezing to below -20°C (Plate 1H). The final melting temperature of the carbonic phase (T_m CO_2) was recorded between -70.0 and -58.2°C (Figure 2A), below the melting point of pure CO_2 (-56.6°C). Melting temperatures below the melting point of pure CO_2 indicate the presence of other dissolved gases in these fluids (*e.g.*, CH_4, N_2). Homogenization of the carbonic phase (T_h CO_2) occurred to the liquid phase over a wide temperature range (-0.5 to 20.7°C; Figure 2B), indicating highly variable CO_2 densities. Incorporating the proportion of the carbonic phase of the inclusions at room temperature (fill of 0.1 to 0.7), these homogenization temperatures equate to CO_2 concentrations of ~14 to 61% (Steele-MacInnis, 2018).

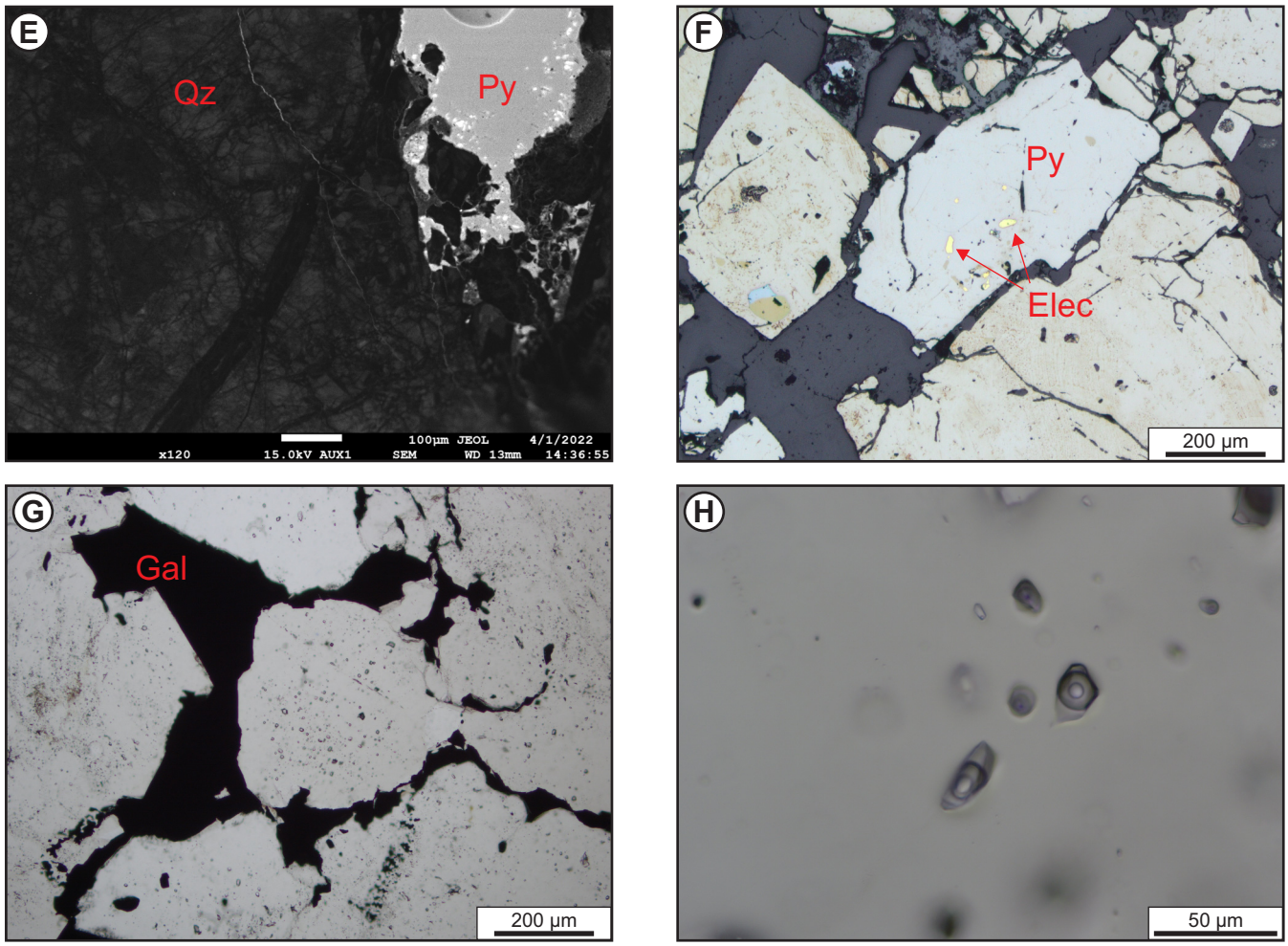

Plate 1 (Continued). *E) Panchromatic cathodoluminescence image of brecciated quartz vein with early quartz (bright luminescence) cut by numerous late quartz veinlets (dull luminescence); F) Electrum inclusions in pyrite grain (sample HS19-072D, RL); G) Cluster of aqueous-carbonic fluid inclusions in quartz grain surrounded by galena (sample HS19-071, PPL; H) Three phase aqueous-carbonic fluid inclusions in FIA of indeterminate origin, sample HS19-070E (@ 0°C). All mineral abbreviations are from Whitney and Evans (2010).*

Clathrate melting was observed in some inclusions prior to homogenization of the carbonic phase between 3.4 and 7.2°C and were used to calculate fluid salinities of 4.6 to 11.3 eq. wt. % NaCl. This is considered a slight underestimate due to the possible presence of CH_4 which extends the stability field of clathrate (Diamond, 1994). Upon further heating most inclusions decrepitated between 300 and 350°C, due to the high internal pressures of the aqueous-carbonic fluids. Total homogenization temperatures (T_h tot) were recorded in nine fluid inclusions between 280.7 and 383.8°C (Figure 2D).

In some FIAs, carbonic inclusions with no aqueous component and two-phase (liquid + vapour) inclusions were observed in the same FIA, suggesting fluid immiscibility. Carbonic inclusions have final melting temperature of -57.5 and -63.7°C (Figure 2A) and homogenized to the liquid phase between -11.3 and 25.9°C, consistent with highly variable fluid densities and the presence of gases other than CO_2 (*e.g.*, CH_4, N_2). Two-phase inclusions do not display T_m CO_2 or T_h CO_2, but the observation of clathrate melting between 4.8 and 7.9°C indicate the presence of small amounts of dissolved carbonic gases in the vapour phase (calculated X_{CO2} of ~0.03; Figure 2C). Clathrate melting temperatures were also used to calculate salinities of 6.4 to 11.7 eq. wt. % NaCl. These inclusions have lower total homogenization temperatures than three-phase inclusions (225.0 to 257.8°C).

Microthermometric measurements from three phase inclusions were used to calculate isochores for individual fluid inclusions using the spreadsheet provided by Steele-

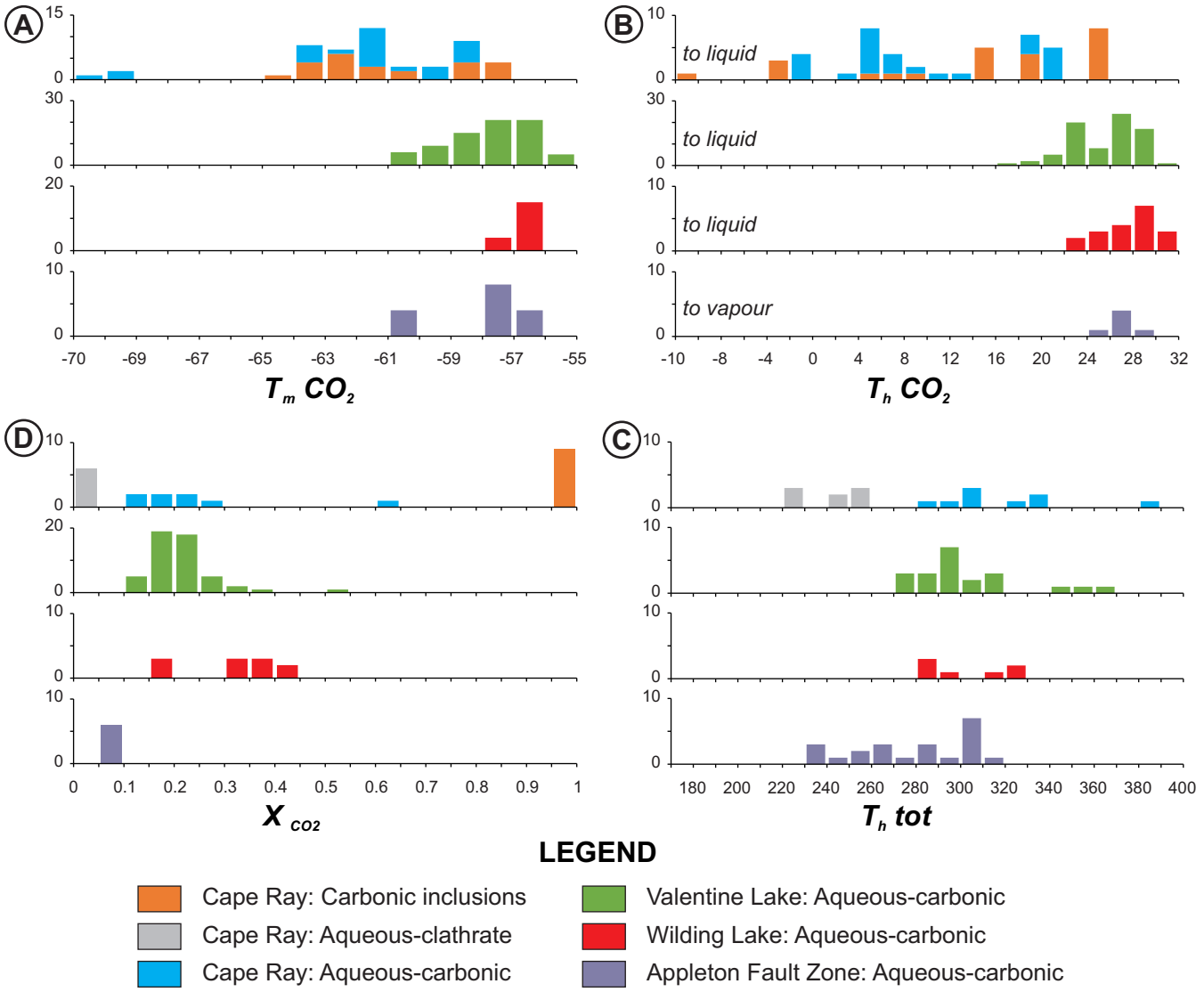

Figure 2. *Histograms of microthermometric data collected during this study. A) Melting temperature of carbonic phase; B) Homogenization temperature of the carbonic phase to the liquid and vapour phase; C) Calculated volume fraction of the carbonic phase; D) Total homogenization temperature.*

MacInnis (2018). Isochores indicate trapping pressures from ~2.77 to 3.71 kbars at 350°C and 4 to 5.88 kbars at 500°C.

Sulphur-Isotope Studies

In-situ sulphur-isotope data were obtained from nine pyrite grains in three samples, two from the Central Zone Deposit (51 Zone) and one from the Windowglass Hill Deposit (Table 3). Samples from the Central Zone Deposit have relatively consistent average $\delta^{34}S$ values of 0.9 ± 1.5‰ and 1.23 ± 3.8‰. However, within some individual pyrite grains there are significant variations in ^{34}S values, with standard deviations of up to 5.4‰. Pyrite grains in the Windowglass Hill Deposit generally have higher $\delta^{34}S$ values (average 3.4 ± 3.2‰), but there are also significant inter- and intra-grain variations with measured values of -2.1 ± 1.1 to 5.1 ± 3.2‰ (Table 3, Figure 3). These values are similar to previously published, bulk sulphur isotope data from pyrite grains at Cape Ray (Wilton and Strong, 1986), which are 0.4 ± 6.4‰ for the Central Zone Deposit and 4.2 ± 1.2‰ for the Windowglass Hill Deposit.

VALENTINE LAKE DEPOSITS

The Valentine Lake deposits in central Newfoundland (Figure 1) consist of five separate gold deposits (Leprechaun, Sprite, Berry, Marathon and Victory) outlined as open pits, with a combined Measured and Indicated Resource of 3.96 Moz of gold (64.62 Mt at 1.90 g/t Au; Powell *et al.*, 2022). The deposits are structurally controlled

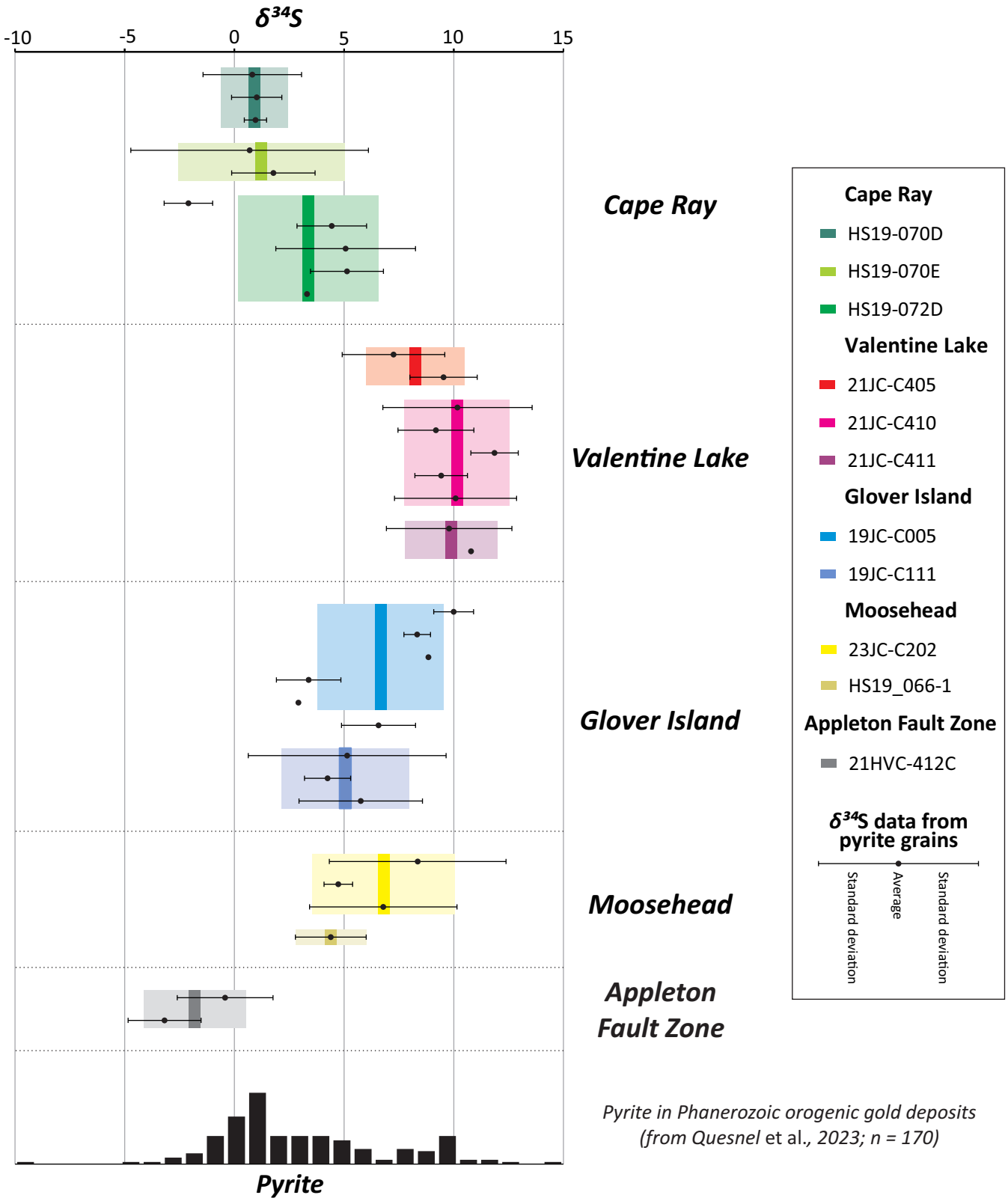

Figure 3. In situ *LA-ICP-MS sulphur isotope data for samples from the Cape Ray, Valentine Lake, Glover Island, Moosehead and Appleton Fault Zone gold occurrences. Shaded areas show average and standard deviation of* $\delta^{34}S$ *data from individual samples. Also included is histogram of sulphur isotope data from pyrite in Phanerozoic orogenic gold deposits (from Quesnel* et al.*, 2023).*

by the Valentine Lake Shear Zone (VLSZ), which is a northwest-dipping, *ca.* 411 Ma backthrust that is interpreted to have reactivated a Late Silurian extensional fault (Honsberger *et al.*, 2022a, b). The VLSZ bounds and uplifts trondhjemite, tonalite, porphyry and gabbro of the Neoproterozoic (*ca.* 570–565 Ma) Valentine Lake Intrusive Suite (Evans and Kean, 2002; Rogers and van Staal, 2002; Rogers *et al.*, 2006) and juxtaposes the Valentine Lake Intrusive Suite with the Silurian Rogerson Lake Conglomerate to the southeast (Honsberger *et al.*, 2022a, b). The Valentine Lake Intrusive Suite is cut by mafic dykes which were emplaced during deformation in the VLSZ, but before gold mineralization (Powell *et al.*, 2022).

Gold mineralization is hosted in quartz–tourmaline–pyrite (QTP) veins that cut trondhjemite, porphyry and mafic dykes (Plate 2A, B) proximal to the sheared contact with the Rogerson Lake Conglomerate (Powell *et al.*, 2022). Two main vein sets have been identified (Powell *et al.*, 2022), a dominant set of shallowly southwest-dipping, en-echelon extension veins at a high angle to the regional foliation, and a lesser set of steeply northwest-dipping to subvertical fault-fill veins parallel to the regional foliation. Alteration of the host plutonic rocks is variable, with narrow zones around mineralized veins characterized by Na-alteration of plagioclase (Layne *et al.*, 2023). The age of the auriferous mineralization is poorly constrained by a *ca.* 411 Ma chemical abrasion-isotope dilution-thermal ionization mass spectrometry (CA-ID-TIMS) U–Pb age on rutile from an auriferous QTP vein (Honsberger *et al.*, 2022a) and a *ca.* 377 Ma ID-TIMS U–Pb age for hydrothermal monazite in mineralized quartz (Layne *et al.*, 2023); both from the Leprechaun Pond deposit. An $^{40}Ar/^{39}Ar$ step-heating age on a multigrain muscovite separate from auriferous drillcore yielded a quasi-plateau age of 384.2 ± 1.6 Ma (Sandeman *et al.*, 2022), comparable to the monazite age.

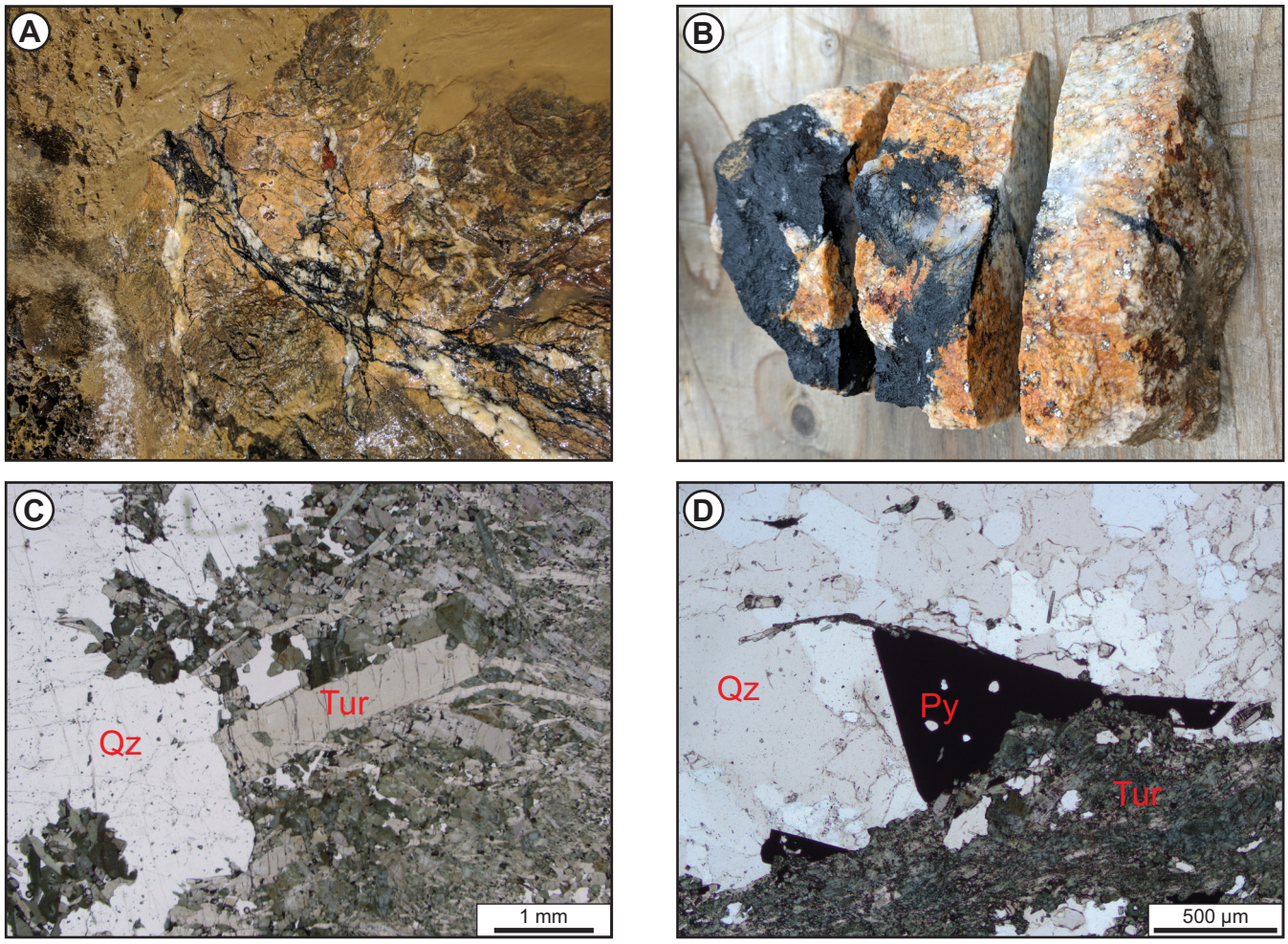

Plate 2. *Representative photographs and photomicrographs from Valentine Lake deposits. A) Valentine Lake Intrusive Suite cut by quartz–tourmaline–pyrite (QTP) veins, Victory Deposit; B) Typical QTP vein sample, Marathon Deposit; C) QTP vein with euhedral to subhedral tourmaline and clear quartz (sample 21JC-C412, PPL); D) Euhedral pyrite, fine-grained tourmaline and medium- to coarse-grained quartz in QTP vein (sample 21JC-C410, PPL).*

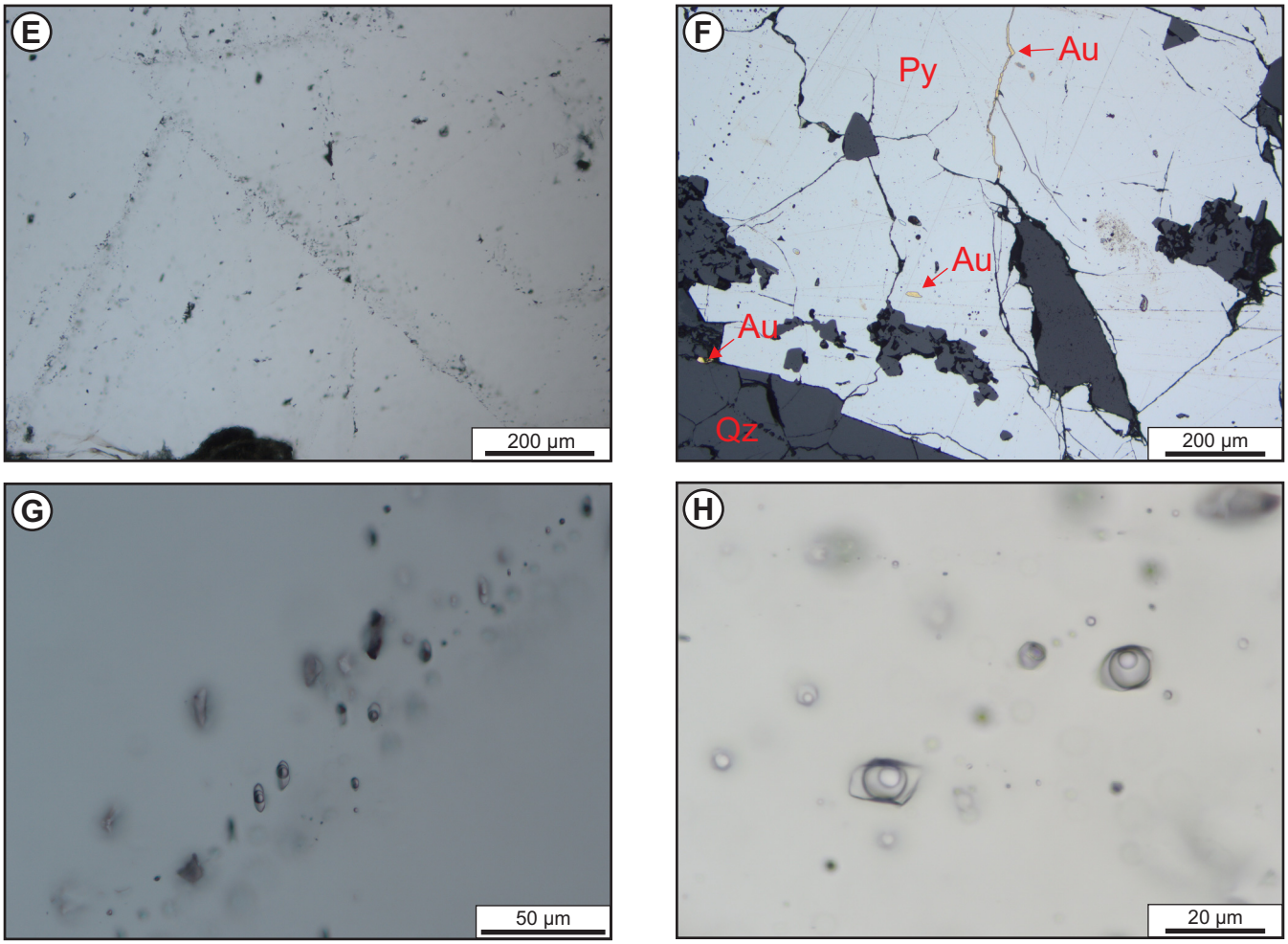

Plate 2 (Continued). *E) Clear, coarse-grained quartz with well-developed growth zone hosting primary FIA (sample 21JC-C405, PPL); F) Gold grains as inclusions in pyrite, in quartz and in late fractures (sample 21JC-C410, RL); G) Primary FIA along growth zone in quartz crystal, with three-phase aqueous-carbonic fluid inclusions (sample 21JC-C405, PPL); H) Large three-phase aqueous-carbonic fluid inclusions in FIA of indeterminate origin (sample 21JC-C410, PPL). All mineral abbreviations are from Whitney and Evans (2010).*

Vein Petrography

Six QTP veins were sampled from diamond-drill core at Valentine Lake, three from the Leprechaun Deposit, two from the Marathon Deposit and one from the Berry Deposit (Table 1). All samples come from intervals with greater than 0.5 g/t Au. The veins are relatively undeformed and predominantly consist of coarse- to medium-grained quartz, clots and veins of fine- to medium-grained acicular tourmaline and euhedral to subhedral pyrite (Plate 2C, D). The quartz is relatively undeformed with only weak undulose extinction and no evidence of significant recrystallization and has a uniform dull fluorescence under CL. Larger quartz grains display well developed growth zones marked by trails of primary fluid inclusions (Plate 2E). Minor calcite is recorded in some samples, as well as trace accessory monazite and rutile. Pyrite is the only sulphide recorded in these samples, although Barrington *et al.* (2016) report pre-native gold precious-metal–telluride and post-native gold–base-metal–telluride assemblages in mineralized veins. Rare chalcopyrite, pyrrhotite, sphalerite and galena-rich quartz veins also occur locally and appear to be late in the paragenetic sequence (Barrington *et al.*, 2016; Powell *et al.*, 2022). Gold is associated with pyrite grains in QTP veins, occurring as discrete grains on the margins or surrounded by pyrite and in late-stage fractures (Plate 2F).

Fluid-inclusion Studies

Fluid inclusions were analyzed in five samples, two from the Leprechaun Deposit, two from the Marathon Deposit, and one sample from the Berry Deposit (Table 2).

Quartz is generally clear and primary FIAs were observed in growth zones (Plate 2E) as well as FIAs of indeterminate origin in clear quartz grains associated with sulphides. Some decrepitated inclusions were noted, but evidence of post-entrapment modification is rare. FIAs of all types contain three-phase aqueous-carbonic fluid inclusions at 0°C (Plate 2G, H). $T_m CO_2$ occurred between -60.3 and -55.7°C, indicating compositions ranging from pure CO_2 to CO_2 with minor other gas phases (*e.g.*, CH_4, N_2). Homogenization of the carbonic phase to the liquid phase occurred between 16.3 and 30.1°C (Figure 2B) and combined with the proportion of the carbonic phase at homogenization was used to calculate X_{CO2} of 0.12 to 0.54. Clathrate melting occurred between 3.4 and 8.7°C and was used to calculate fluid salinities of 2.6 to 11.4 eq. wt. % NaCl. Decrepitation of inclusions prior to total homogenization was common (between 200 and 340°C). Where total homogenization of the inclusions was recorded, it occurred with the liquid, vapour and critical phases (dependent of the proportion of the carbonic phase) between 275 and 364.1°C (Figure 2D). Isochores constructed using the spreadsheet of Steele-MacInnis (2018) indicate trapping pressures from 2.42 ± 0.39 kbars at 350°C and 3.73 ± 0.62 kbars at 500°C.

Sulphur-isotope Studies

Seven pyrite grains in three samples were selected for *in-situ* LA-ICP-MS sulphur isotope analysis (Table 3), with data for the cores and rims obtained from three grains. These data show relatively consistent average $\delta^{34}S$ values in all pyrite grains, ranging from 7.3 ± 2.3‰ to 11.9 ± 1.1‰ (Table 3, Figure 3). There is no systematic change in $\delta^{34}S$ values between the cores and rims of crystals, with minor shifts to both positive and negative $\delta^{34}S$ values recorded (Table 3). The ^{34}S values derived in this study are consistent with a single previously reported bulk $\delta^{34}S$ value of 10.7‰ from a pyrite grain at Valentine Lake (Evans and Wilson, 1994).

WILDING LAKE PROSPECTS

The Wilding Lake prospects are located approximately 30 km northeast of the Valentine Lake deposits, along the northeastern extension of the VLSZ (Figure 1; Honsberger *et al.*, 2019a). There, eight gold showings have been discovered in the footwall of the VLSZ, with exploration highlights from diamond drilling in 2017 including 10.01 g/t over 5.35 m at the Elm Zone and 2.02 g/t over 4.90 m at the Alder Zone (Evans, 2020). Unlike the Valentine Lake deposits, gold mineralization at Wilding Lake is hosted by *ca.* ≤421 Ma Rogerson Lake Conglomerate (Alder and Elm zones) and *ca.* 422 Ma feldspar porphyry and felsic volcanic flows (Honsberger *et al.*, 2019a, 2022a) at the Red Ochre zone and Third Spot showing, respectively.

Detailed structural mapping of exposed quartz veins at the Elm and Alder zones has identified multiple sets of veins within an oblique sinistral reverse shear zone that involved a component of north-northeast-directed thrusting (Honsberger *et al.*, 2019a, b). The main veins are laterally extensive quartz veins that dip moderately to the southeast, with moderately dipping extensional veins extending from the main veins into the altered conglomerate. Younger sets of steeply dipping tourmaline-bearing and chalcopyrite-rich extensional veins cut earlier vein generations (Plate 3A, B) and indicate transient phases of horizontal extension and dextral transpression (Honsberger *et al.*, 2019a, b). Gold mineralization is found locally in all vein sets but is more abundant in the younger steeply dipping veins.

Vein Petrography

Five quartz vein samples were analyzed from Wilding Lake, two from the Alder Zone and three from the Elm Zone (Table 1). All vein samples are mineralized, with gold grades of up to 4.9 g/t Au at the Alder Zone and up to 25.5 g/t Au at the Elm Zone. Chalcopyrite-rich veins also contain significant Cu, up to 28.1% Cu in sample HS18-115 from the Elm Zone.

The samples from the Alder Zone were collected from a chalcopyrite bearing zone of the main vein (V1: HS18-129B) that is cut by a steeply dipping tourmaline-bearing vein (V2: HS18-129A). The main vein consists predominantly of fine- to medium-grained quartz cut by thin veinlets of pyrite and chalcopyrite that are locally almost completely replaced by goethite. The tourmaline-bearing vein consists of coarse-grained, strongly deformed quartz grains with undulose extinction, and thin (<5 mm) layers of fine-grained quartz, acicular tourmaline and minor aggregates of altered sulphide minerals (replaced by goethite). No visible gold was observed in these samples.

Samples from the Elm Zone were collected from a set of steeply dipping laminated chalcopyrite-bearing veins (V_2) that cut the main vein (V_1); the former which hosts the highest gold grades in this zone (Honsberger *et al.*, 2019b). These samples are composed of coarse- to medium-grained gangue quartz, euhedral to subhedral pyrite and chalcopyrite (Plate 3C–E) and minor siderite, muscovite, chlorite and fine-grained intergrowths of rutile and Fe-oxides. Abundant gold and electrum grains occur as inclusions in pyrite and chalcopyrite and in quartz (Plate 3E). Late-stage supergene alteration of the veins is extensive, with pyrite and chalcopyrite replaced by goethite and hematite along fractures (Plate 3C, D). Secondary supergene minerals also include abundant malachite infilling secondary porosity and minor hessite (Ag_2Te), lenaite ($AgFeS_2$), fischesserite (Ag_3AuSe_2),

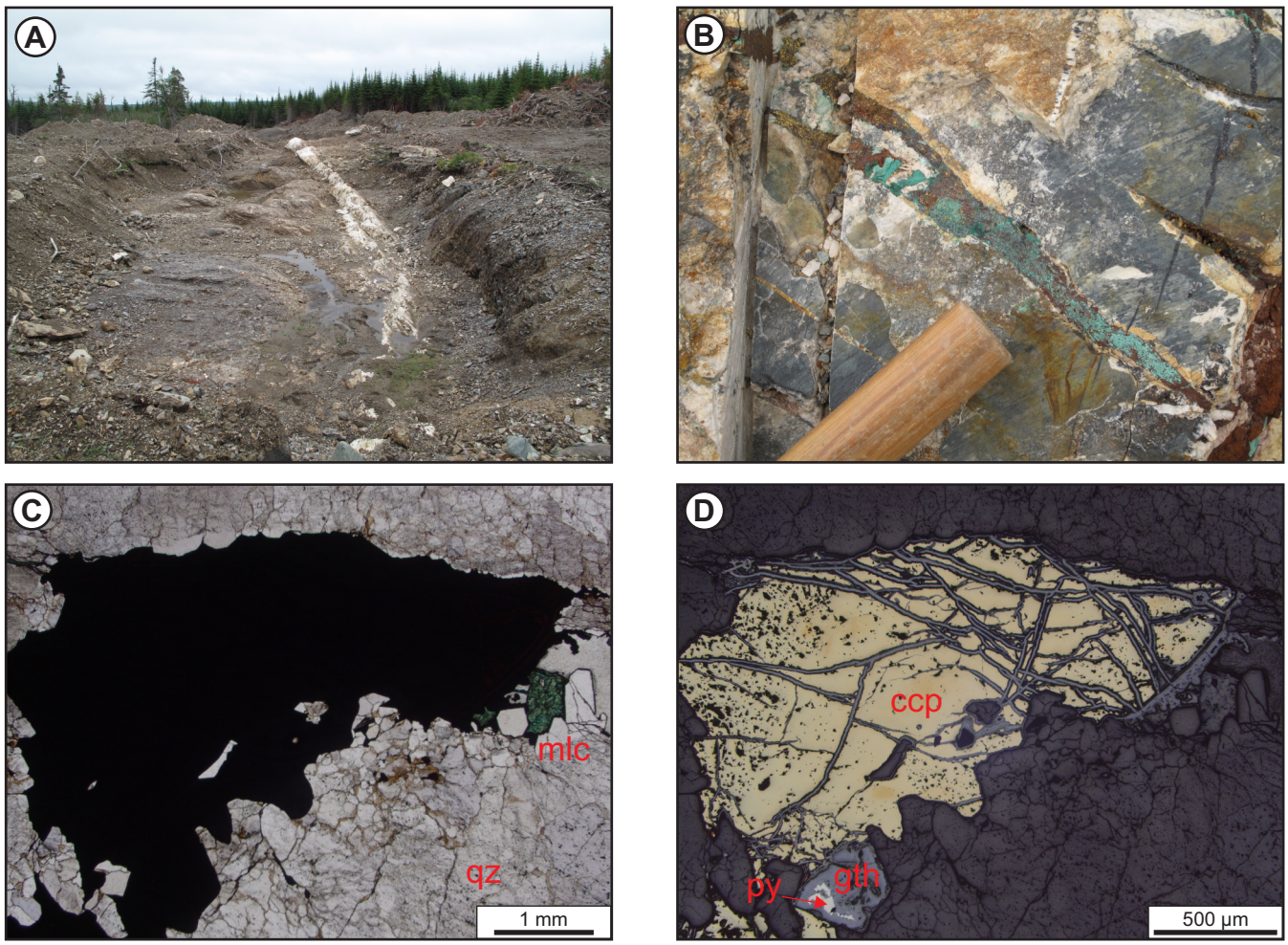

Plate 3. *Representative photographs and photomicrographs from the Alder and Elm zones at Wilding Lake. A) Main shear vein (V1) cutting Rogerson Lake Conglomerate, Elm Zone; B) Tourmaline-bearing vein (V2) cut by chalcopyrite-rich vein (V3), Alder Zone; C) Mineralized vein with chalcopyrite and pyrite in recrystallized quartz with secondary malachite (sample HS18-115, PPL); D) Same view as C) in RL, showing pervasive alteration of pyrite and chalcopyrite to goethite along fractures.*

acanthite (Ag_2S) and unnamed Ag–Au–Bi tellurides in goethite veins or replacing pyrite and chalcopyrite.

Fluid-inclusion Studies

Gangue quartz in all samples is characterized by a high abundance of fluid inclusions (Plate 3F) and commonly show evidence for post-entrapment modification (leaking, necking down, decrepitation). In addition, quartz is commonly recrystallized to fine-grained quartz during late structural modification, and larger quartz grains have parallel arrays of late secondary fluid inclusions (Plate 3G) which likely formed during late deformation (Tuba *et al.*, 2021). Rare primary FIAs in growth zones and cores of quartz grains, and FIAs of indeterminate origin were recorded in clear quartz associated with sulphides and are interpreted to represent fluid present during gold deposition.

Fluid inclusions were analyzed in two samples from the Elm Zone (Table 2). Fluid inclusions in primary and indeterminate FIAs are three-phase aqueous-carbonic inclusions (Plate 3H). Melting of the carbonic phase occurred between -57.1 and -56.6°C (Figure 2A), close to the melting temperature of pure CO_2 (-56.6°C), indicating only minor amounts of gases other than CO_2. The carbonic phase homogenizes to the liquid phase between 23.5 and 30.7°C and when combined with the proportion of the carbonic phase after homogenization, corresponds to X_{CO2} of 0.17 to 0.42 (Figure 2C). Clathrate melting between 7.6 and 8.9°C corresponds to fluid salinities of 2.2 to 4.7 eq. wt. % NaCl. Total homogenization occurred to the vapour phase between 285 and 325°C, with many inclusions decrepitating prior to total homogenization. Calculated isochores for FIAs indicate trapping pressures of 1.89 ± 0.34 kbars at 350°C and 2.90 ± 0.57 kbars at 500°C.

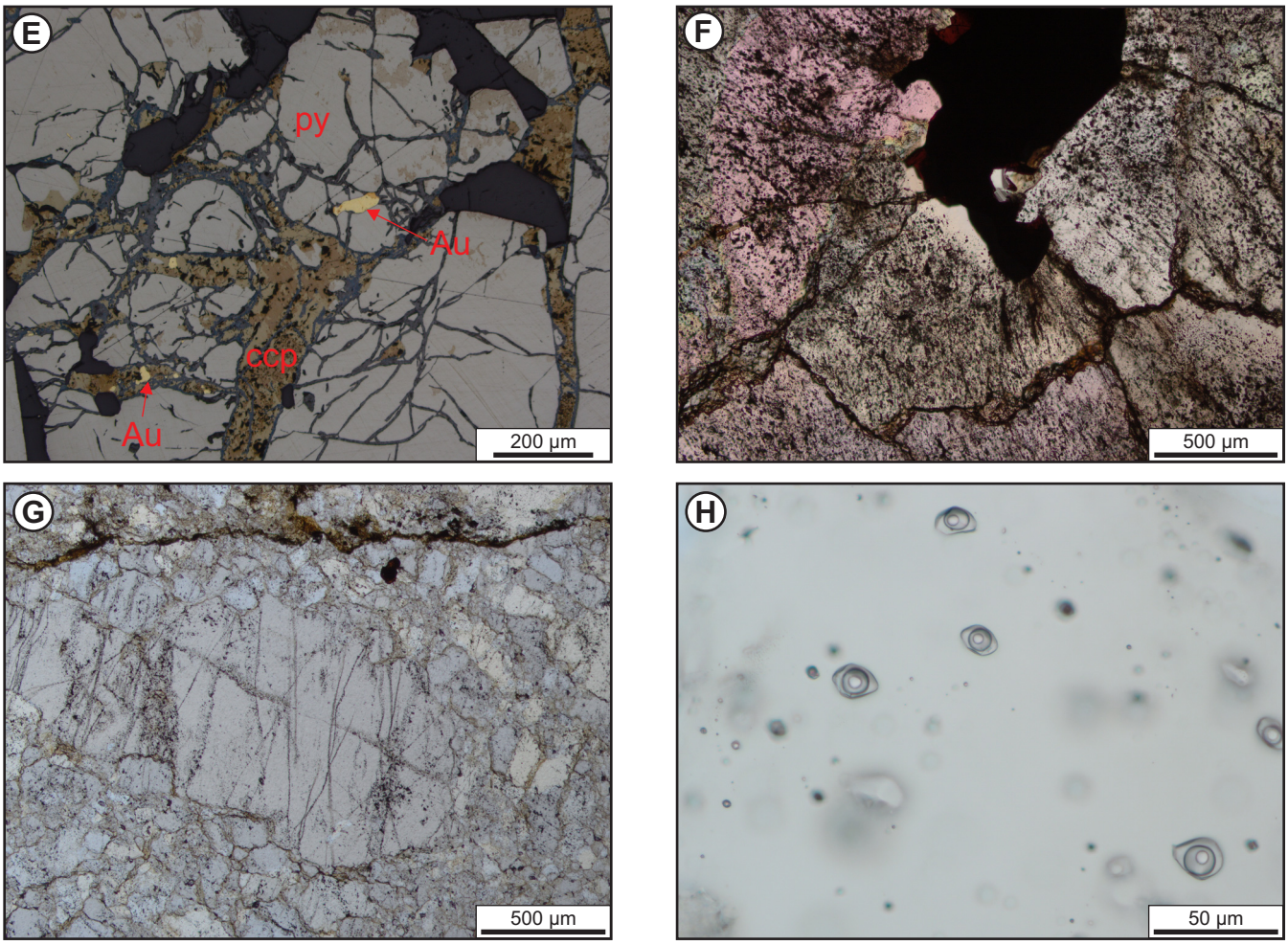

Plate 3 (Continued). *E) Fractured and altered pyrite and chalcopyrite with discrete gold grains (sample HS18-115, RL); F) Quartz inundated by fluid inclusions giving a dark cloudy appearance and making identification of FIAs impossible (sample HS18-130E, PPL); G) Large quartz grain with sub-parallel trails of secondary FIAs formed during ductile deformation, surrounded by fine-grained recrystallized quartz (sample HS18-130B, PPL); H) Three-phase aqueous-carbonic fluid inclusions in FIA of indeterminate origin (sample 21JC-C410, PPL). All mineral abbreviations are from Whitney and Evans (2010).*

GLOVER ISLAND DEPOSITS

Glover Island in western Newfoundland is located along the boundary between the Notre Dame Subzone and the Humber Zone, with the boundary marked by the Baie Verte Brompton Line–Cabot Fault Zone (BCZ; Williams and St. Julien, 1982; Brem, 2007). Exploration from the 1980s to 2012 has identified multiple gold prospects over a strike length of >7 km (Barbour *et al.*, 2012), including the Lunch Pond South East (LPSE) deposit which has a NI 43-101 Indicated Mineral Resource of 58 200 oz. gold and an additional Inferred Mineral Resource of 120 600 oz. gold (Puritch and Barry, 2017). All gold prospects occur within 5 km of the BCZ and are hosted in volcanic and sedimentary rocks of the Cambro-Ordovician Glover Group, which forms the cover sequence to the Grand Lake Ophiolite Complex (Conliffe, 2021, 2022).

Gold mineralization has been classified into two types based on the style of mineralization and host lithologies (Conliffe, 2021). Volcanic-hosted mineralization is the predominant type, with mineralized veins occurring in strongly deformed and altered felsic to mafic tuffs and rhyolites of the Late Ordovician Kettle Pond Formation, which forms kilometre-scale fold nappes in probable Salinic thrust sheets (Barbour *et al.*, 2012; Conliffe, 2021). Mineralized units typically are associated with thrust surfaces (Barbour *et al.*, 2012) and are brecciated with multiple generations of quartz veins. In some areas, intense silicification and brecciation imparts a distinctive “chicken-wire” texture (Plate 4A)

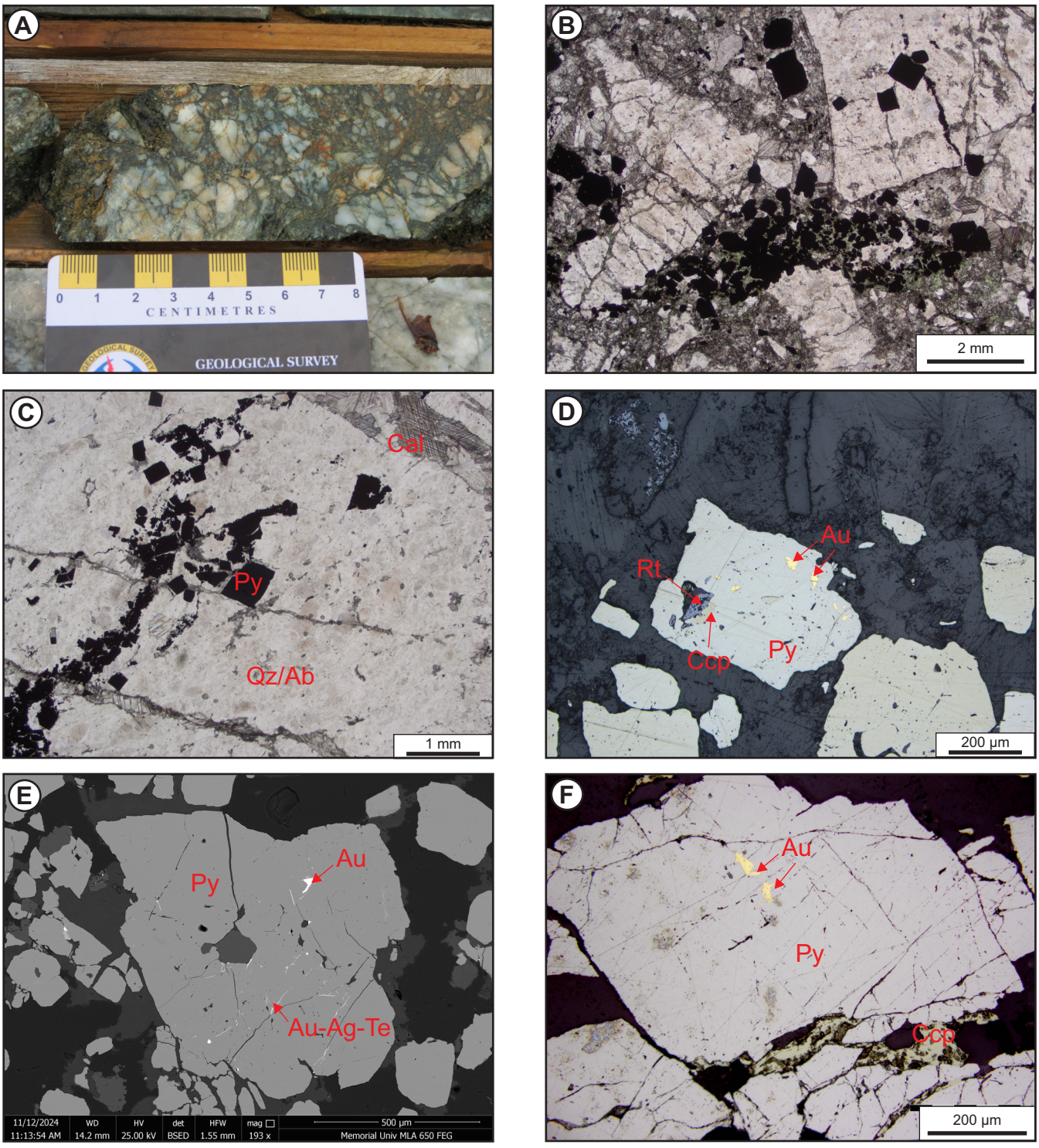

Plate 4. *Representative photographs and photomicrographs from gold zones on Glover Island. A) "Chicken-wire" breccia in mineralized quartz vein at the LPSE Deposit (drillhole LPSE-1 @ 38.3 m); B) Brecciated quartz vein with large quartz clasts in matrix of calcite, albite, chlorite, pyrite and quartz (sample 19JC-C005, PPL); C) Brecciated quartz vein cut by late calcite veinlets (sample 19JC-C111, PPL); D) Pyrite grain with inclusions of gold, chalcopyrite and rutile (sample 19JC-C005, RL; E) SEM image of pyrite grain with gold inclusions and Au–Ag tellurides in late fractures (sample 19JC-C030); F) Pyrite and chalcopyrite in mineralized quartz vein, with gold inclusions in pyrite (sample 19JC-085-A01, RL); All mineral abbreviations are from Whitney and Evans (2010).*

formed by thin seams of chlorite and pyrite (± carbonate ± albite) cementing quartz and albite vein fragments. Mineralized zones are surrounded by intense, proximal (<5 m), quartz–albite–sericite–carbonate–pyrite–chlorite alteration, with alteration decreasing to a distal chlorite ± carbonate ± sericite alteration that grades into the background regional metamorphic mineral phases (Conliffe, 2021). Mineralization has also been recorded in folded conglomerate units at the base of the Kettle Pond Formation (conglomerate-hosted mineralization) and occurs in decametre-scale massive white quartz (± pyrite) veins (Conliffe, 2021). This mineralization style is characterized by high gold grades (up to 150 g/t over 1.5 m), but veins are discontinuous and have not been intercepted during subsequent drilling (Barbour *et al.*, 2012).

Radiometric ages are lacking for the Glover Island deposits, but structural evidence shows that mineralization occurred syn- to post-D_2 deformation but pre-D_3 deformation (Barbour *et al.*, 2012; Conliffe, 2021) and Brem (2007) considered that this deformation occurred during the latest stages of the Silurian Salinic orogeny at ~420 Ma. Similar structural relationships between orogenic gold mineralization and late Salinic deformation have been reported from the Baie Verte Peninsula close to the BCZ (Castonguay *et al.*, 2009), and geochronology indicates that gold mineralization at Baie Verte occurred at *ca.* 420 Ma (Ramezani *et al.*, 2000; Castonguay *et al.*, 2009; Mănuc, 2023).

Vein Petrography

Four samples from Glover Island were selected for detailed petrographic analysis, three examples from volcanic-hosted mineralization (two from the LPSE Deposit and one from the Kettle Pond South Prospect) and one from the conglomerate-hosted mineralization at the Lunch Pond Prospect (Table 1). These samples are characterized by high gold grades ranging from 6.5 to 44.2 g/t Au.

Mineralized veins from volcanic-hosted mineralization are characterized by clasts of strongly deformed and recrystallized early quartz and fine-grained quartz–albite in a matrix of calcite, albite, chlorite, pyrite, ankerite, rutile, apatite and trace zircon, titanite and monazite (Plate 4B). Late-stage calcite veins crosscut earlier breccia zones (Plate 4C). Gold grains are common and occur as inclusions in pyrite grains (Plate 4D, E). Gold is Ag poor with EDS spectra indicating Ag contents of 1.2 to 5%. Pyrite grains were brecciated during late brittle deformation, and galena and Au–Ag–Pb sulphides and tellurides are recorded as micro-inclusions in pyrite, and/or in late fractures in brecciated pyrite (Plate 4E).

Mineralized quartz veins in conglomerate-hosted mineralization do not display the intense brecciation observed in volcanic-hosted mineralization. Gangue quartz is coarse-grained with undulose extinction and is crosscut by numerous trains of secondary fluid inclusions. Mineralization is confined to aggregates of pyrite–chlorite–albite–muscovite–chalcopyrite with trace amounts of apatite and rutile. Gold grains occur as inclusions in pyrite (Plate 4F) and are also associated with chalcopyrite in late fractures in brecciated pyrite grains. SEM-MLA analysis also identified inclusions of galena, bismuth tellurides and coaslite ($Pb_2Bi_2S_5$) in pyrite, spatially associated with gold grains. No suitable FIAs for microthermometric analysis were identified, due to the strong deformation and recrystallization, and the high abundance of secondary fluid inclusion trails.

Sulphur-isotope Studies

Sulphur-isotope data were collected from six pyrite grains in two samples from the LPSE deposit (Table 3, Figure 3). These data show a broadly bimodal distribution, and in sample 19JC-C005 a clear distinction in $\delta^{34}S$ is discernable between the cores and rims of the pyrite grains. The cores of pyrite grains have $\delta^{34}S$ values of 4.4 ± 2.1‰, with the rims showing a shift to isotopically heavier $\delta^{34}S$ (9.0 ± 1.0‰). In sample 19JC-C111 the $\delta^{34}S$ values for three pyrite grains range from 4.2 ± 1.1‰ to 5.8 ± 2.8‰.

MOOSEHEAD PROSPECT

The Moosehead gold prospect is located ~3 km southeast of the town of Bishops Falls, in central Newfoundland, approximately 11 km southeast of the Northern Arm Fault and ~140 km northeast and along strike of the VLSZ (Figure 1). The Moosehead Prospect is host to significant quartz vein-hosted gold mineralization which has been encountered over a strike length of 2 km, with recent drilling highlights including 11.90 m @ 44.96 g/t Au (Eastern Trend), 39.60 m @12.50 g/t Au (463 Zone), and 5.64 g/t over 5.94 m at the recently discovered 552 Zone, lying ~2 km to the southeast of the main mineralized zone (Sokoman Minerals Corp. website). The Moosehead property is mostly underlain by openly folded and likely imbricated sedimentary rocks of the <428 Ma (Honsberger *et al.*, 2022b) Wigwam Formation of the Botwood Group, consisting of variably coloured muscovite-bearing sandstones, siltstones, and lesser argillites (Dickson *et al.*, 2000; Barbour, 2004; Morgan, 2016; Sandeman and Honsberger, 2023). Mafic and silicic volcanic rocks along with sparse cobble to pebble conglomerates of the lower Botwood Group (Laurenceton Formation) occur immediately south and southeast of the prospect, and *ca.* 429 Ma felsic volcanic rocks of the Charles Lake belt occur to the southwest (Honsberger *et al.*, 2022b). Quartz veined intervals are commonly associated with, or occur proximal to, multi-metric-scale horizons of strongly cleaved and brecciated graphitic black shale of

unknown age. Diamond drilling, in combination with magnetic intensity maps, illustrates that numerous fine- to medium-grained, moderately to strongly magnetic mafic dykes of unknown age cut the Late Silurian host rocks.

The Moosehead vein systems occur in a series of north-northwest-directed thrust panels containing rocks of the Early to Middle Silurian Badger Group, the Middle to Late Silurian Botwood Group (Laurenceton and Wigwam formations; Dickson *et al.*, 2000) and possibly the latest Ordovician to earliest Silurian black shale of the Lawrence Harbour Formation (and equivalents; Boyce *et al.*, 1991; Williams, 1989, 1993). Four kilometres east of the Moosehead property, the Mount Peyton Intrusive complex (Blackwood, 1982; Strong, 1979; Sandeman *et al.*, 2017), an ovoid, largely bimodal, Ludlow to Lochkovian aged gabbroic to monzogranitic intrusion, cuts the rocks of the Badger Group, forming a syn-kinematic metamorphic halo around the intrusive complex. The north-northwest-directed thrust panels are cut by a series of north-northwest-trending auriferous quartz veins that form the bulk of the mineralization at Moosehead. East–west oriented dextral normal faults cut the imbricated sequences, and these may offset the mineralized structures.

Gold mineralization is hosted in a series of extensional, moderately east dipping quartz–carbonate veins (Plate 5A, B), that cut earlier, barren to weakly mineralized quartz–ferroan dolomite–sulphide veins and are in turn cut by later, barren quartz–carbonate veins (Barbour, 2004; Conliffe and Wilton, 2009; Morgan, 2016; Sandeman and Honsberger, 2023). The Moosehead orogenic vein system postdates intrusion of the mafic dykes and folding of the Wigwam Formation, and therefore likely formed at ≤ *ca.* 411 Ma, the

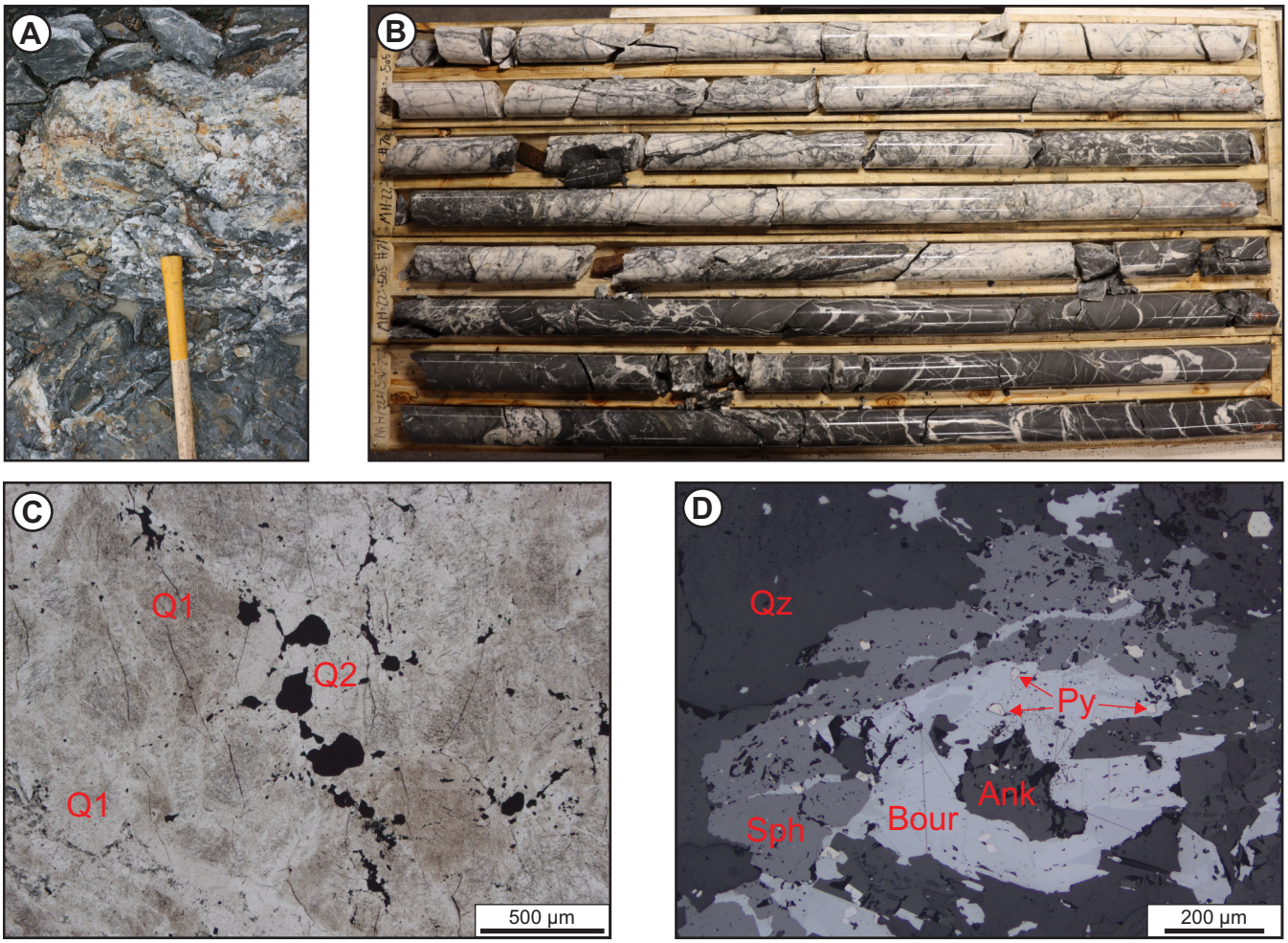

Plate 5. *Representative photographs and photomicrographs from the Moosehead Prospect. A) Brecciated quartz vein with abundant wall rock fragments, exposed in a trench at Moosehead; B) Mineralized quartz vein from Eastern Trend, displaying breccia textures at margins and abundant stylolites (drillhole MH-22-505 from 203.10 to 214.35 m; C) Brecciated quartz veins with early quartz fragments (Q1) cut by Q2 stylolite containing quartz–ankerite–chalcostibite–galena–pyrite (sample 23JC-C203, PPL); D) Q2 stylolite with bournonite, sphalerite, pyrite, ankerite and quartz (sample 19HS-066_2, RL).*

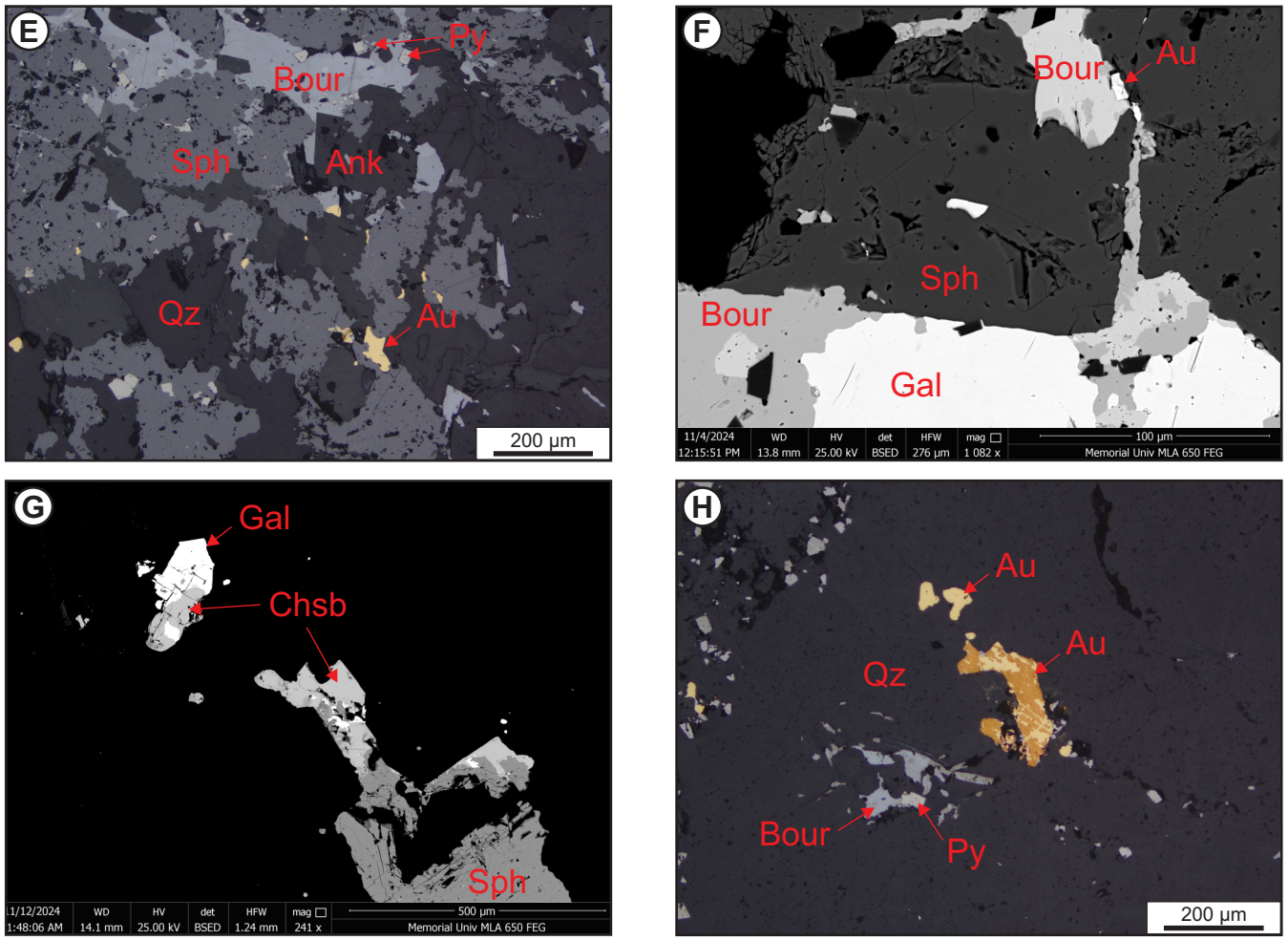

Plate 5 (Continued). *E) Gold grains associated with bournonite, sphalerite, euhedral ankerite and quartz (sample 19HS-066_2, RL); F) SEM image showing complex intergrowth of gold, bournonite, sphalerite and galena (sample 19HS-066_2); G) SEM image showing chalcostibite on the margins of sphalerite and galena grains (sample 23JC-C203); H) Large gold grain in Q2 quartz, spatially associated with bournonite and pyrite (sample 19HS-066_2, RL). All mineral abbreviations are from Whitney and Evans (2010).*

interpreted age of gold mineralization along strike at Valentine Lake and the inferred timing of ductile compressive Acadian imbrication and deformation in north-central Newfoundland (McNicoll *et al.*, 2006; Honsberger *et al.*, 2022a; Sandeman and Honsberger, 2023).

Vein Petrography

Four quartz vein samples were collected from two drillholes in the Eastern Trend Zone at Moosehead (Table 1). These samples come from strongly mineralized zones (5.0 to 55.3 g/t Au) and all contain visible gold. The texturally complex mineralized veins are highly stylolitic, brecciated and occasionally vuggy, and Conliffe and Wilton (2009) identified at least four phases of quartz precipitation, brecciation and recrystallization in mineralized veins (Q1 to Q4). Gold mineralization and associated sulphides and sulphosalts are associated with the main breccia event (Q2 of Conliffe and Wilton, 2009), with mineralized stylolites and associated quartz formed during fluid-enhanced pressure solution.

Petrographic and SEM-MLA analysis show that the samples predominantly contain brecciated gangue quartz (Plate 5C) with minor ankerite and muscovite and trace calcite, epidote, rutile and apatite. Ankerite and muscovite are related to the Q2 brecciation event, and commonly are spatially associated with mineralization (Plate 5D, 5E). Sulphides and sulphosalts occur in Q2 breccia, and consist of pyrite, sphalerite, arsenopyrite, galena, chalcopyrite, and abundant antimony bearing sulphosalts that range in composition from boulangerite ($Pb_5Sb_4S_{11}$) to bournonite

($PbCuSbS_3$) to chalcostibite ($CuSbS_2$). These sulphides and sulphosalts commonly occur as complex intergrowths (Plate 5F, G) and individual grains are locally zoned. Gold occurs as discrete grains in Q2 stylolites with sulphides and sulphosalts (Plate 5F) as well as isolated grains in gangue Q2 quartz (Plate 5H).

Fluid-inclusion Studies

Detailed fluid-inclusion studies at Moosehead were conducted by Conliffe and Wilton (2009) and are summarized here. Careful petrographic analysis identified primary and indeterminate origin FIAs hosted in gangue quartz associated with gold and sulphides/sulphosalt mineralization. These FIAs contain inclusions with a wide range of CO_2 contents (X_{CO2} of <0.05 to 1.00), with three main inclusion types recorded: 1) Carbonic inclusions, in which no aqueous component was observed; 2) Three-phase aqueous carbonic inclusions, forming solid CO_2 on freezing and; 3) Two-phase inclusions forming clathrate but no observable solid CO_2 on cooling. Clathrate melting temperatures and total homogenization temperatures indicate that mineralized veins formed from moderate to high temperature (240–400°C), low to moderate salinity (0–10 eq. wt. % NaCl) aqueous-carbonic fluids, and the wide range of X_{CO2} in individual FIAs is a result of fluid immiscibility during mineralization. Isochore modelling showed that these fluids were trapped at pressures of between 0.72 to 1.55 kbars under hydrostatic to lithostatic conditions (Conliffe and Wilton, 2009).

Sulphur-isotope Studies

Four pyrite grains in two samples from the Moosehead Prospect were selected for sulphur-isotope analysis, with data summarized in Table 3. These data show that $\delta^{34}S$ values are positive but variable, ranging from 4.7 ± 0.7‰ to 8.4 ± 4.0‰ (Figure 3).

DEPOSITS PROXIMAL TO THE APPLETON FAULT ZONE

Gold prospects in the northeastern Exploits Subzone are associated with a ~75 km long structural corridor along the Dog Bay Line and Appleton Fault Zone (Figure 1; Evans, 1996; Honsberger *et al.*, 2023; Sandeman and Honsberger, 2023). The most significant zone of gold mineralization discovered to date lies along the Appleton Fault Zone which is located near the town of Appleton, where recent exploration has reported multiple high-grade deposits with bonanza-style, quartz vein-hosted gold mineralization, and a combined indicated mineral resource of 1.39 Moz (18 Mt at 2.40 g/t) and inferred mineral resource of 0.61 Moz (10.7 Mt at 1.77 g/t Au) (Landry *et al.*, 2025).

Mineralization occurs in siltstone, shale, fine-grained sandstone and greywacke typical of the Hunts Cove and Outflow formations of the Ordovician Davidsville Group, interpreted as representing autochthonous continental margin sedimentary units forming the passive margin of Ganderia (O'Neill and Knight, 1988; O'Neill, 1991; Williams, 1993). These units are weakly to strongly deformed and are locally altered, particularly near fault zones (Honsberger *et al.*, 2023; Sandeman and Honsberger, 2023). Sandeman and Honsberger (2023) interpreted the Appleton Fault Zone in the main mineralized corridor as a moderately to steeply west-dipping high-strain zone characterized by intense fold transposition and brecciation. It appears that the Appleton Fault Zone likely represents the main fluid conduit for the gold mineralized veins.

Gold mineralization occurs in structurally complex domains where quartz veins occupy second-order fracture mesh networks adjacent to the regional structures (Sandeman and Honsberger, 2023). Multiple generations of quartz veins are observed, with early, bedding parallel barren veins and later gold-bearing quartz–carbonate veins which are discordant to regional northeast trending foliation and stratigraphy (Sandeman and Honsberger, 2023; Eccles *et al.*, 2024). Hydrothermal alteration is subtle, with a weak discolouration of the host rock adjacent to the veins locally noted to extend up to 10 m from the vein margins, and changes in mica chemistry from aluminum-rich NH_4 muscovite proximal to mineralized veins to distal phengitic alteration (Eccles *et al.*, 2024). The timing of structurally controlled gold deposition along the Appleton Fault Zone is poorly constrained, but a maximum age of *ca.* 446 Ma was estimated based on the age of mineralized gabbro intrusions within the Ordovician Davidsville Group (Honsberger *et al.*, 2023). It is likely therefore that the vein system near the Appleton Fault Zone represents Middle Devonian arrays generated during transpressive Acadian deformation.

Vein Petrography

Seven quartz–carbonate vein samples from gold deposits along the Appleton Fault Zone were selected for petrographic analysis, two each from the Dome, Keats and Lotto deposits and a single sample from the Big Vein prospect (Table 1). All samples are anomalous in gold, with a maximum gold grade of 3.4 g/t from sample 21HVB-412B (Keats Deposit). Mineralized veins have a wide range of textures, including brecciated, massive-vuggy, laminated, and stock-work styles (Plate 6A). Brecciated veins contain abundant quartz vein and host rock fragments, are cut by rare stylolites (Plate 6B, C), and preserve evidence of multiple phases of quartz precipitation; dissolution and recrystallisation is common in all vein types (Plate 6C). CL imag-

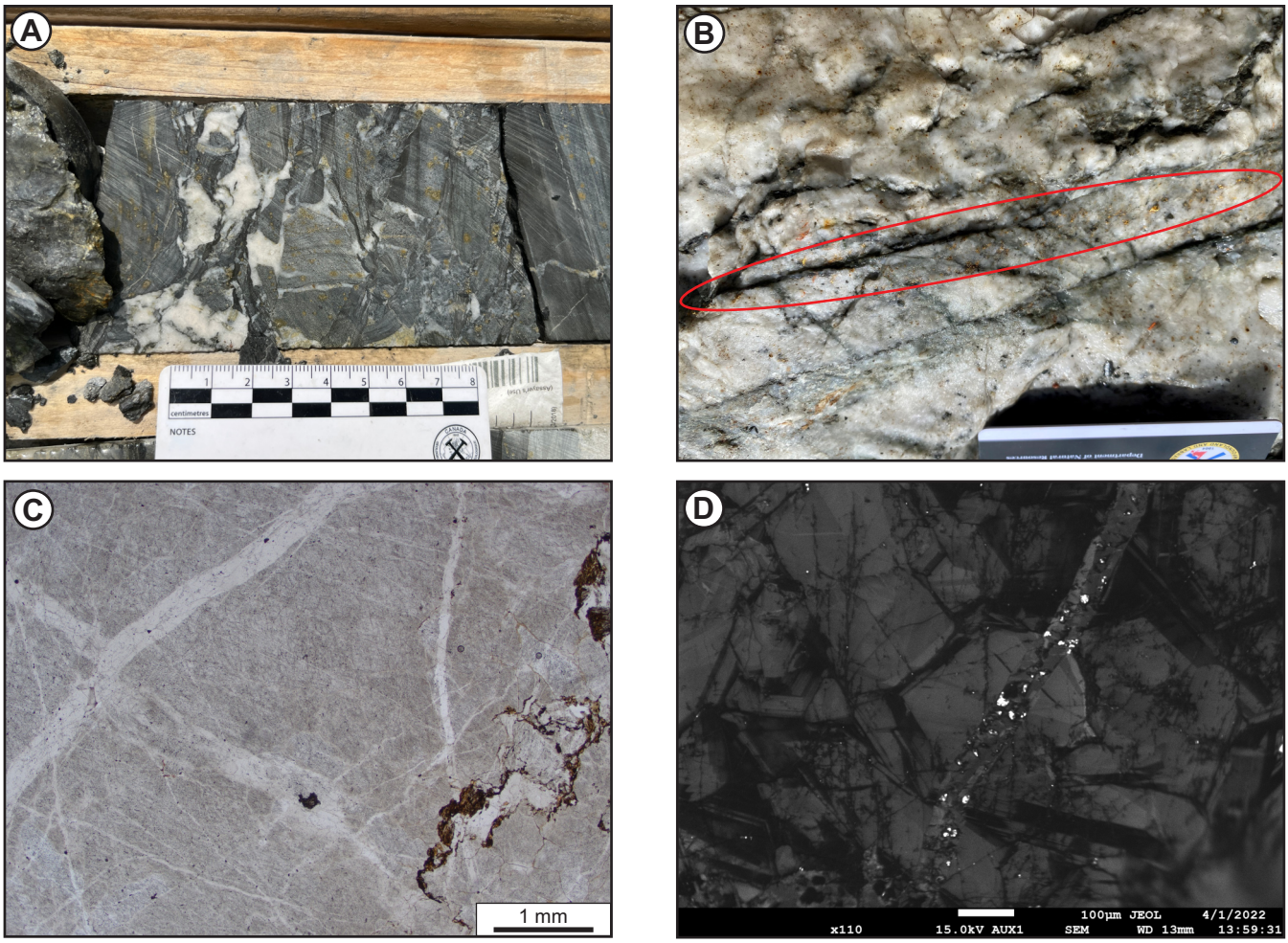

Plate 6. *Representative photographs and photomicrographs from the gold prospects along the Appleton Fault Zone. A) Breccia zone with abundant disseminated arsenopyrite and pyrite in wall rock fragments, Keats Zone; B) Laminated quartz vein with abundant gold mineralization along stylolite (pressure dissolution seam), Keats Zone; C) Brecciated quartz vein with early quartz fragments cemented by later clear quartz (sample Big Vein 2, PPL); D) Panchromatic cathodoluminescence image of early quartz (bright luminescence) cut by numerous late quartz veinlets (dull luminescence), and abundant sulphides (bright spots) in late quartz (sample Lotto Vein 1).*

ing highlighted distinct internal zoning in early quartz fragments, which are in turn crosscut by thin stockwork-style quartz veinlets that occasionally contain fine sulphides (Plate 6D).

Host-rock fragments (shale and siltstone) contain abundant disseminated pyrite and arsenopyrite. Veins consist predominantly of quartz and ankerite with trace muscovite, chlorite, albite, calcite, rutile and monazite. Sulphides and sulphosalts are disseminated in quartz or are associated with minor stylolites, and include pyrite, arsenopyrite, boulangerite, chalcostibite and chalcopyrite (Plate 6E). Gold was only observed in one sample from the Dome Deposit (21HVB-421D), where it is associated with tetrahedrite and an unknown Ni–Au–Sb mineral (Plate 6F).

Fluid-inclusion Studies

Multiple quartz generations are present in the mineralized veins, with petrographic and optical CL analysis revealing a complex history of brecciation, quartz precipitation and recrystallization (Plate 6C, D). In addition, samples are characterized by a high abundance of fluid inclusions representing multiple fluid flow events, and fluid inclusions commonly show evidence of post-entrapment modification and pressure fluctuations, such as decrepitated inclusions with well-developed halos of neonate inclusions (Plate 6G; Zoheir *et al.*, 2019, Tuba *et al.*, 2021). This makes identification of primary FIAs associated with the main mineralization event difficult, and most samples analyzed did not have suitable FIAs for microthermometric analysis. Suitable FIAs

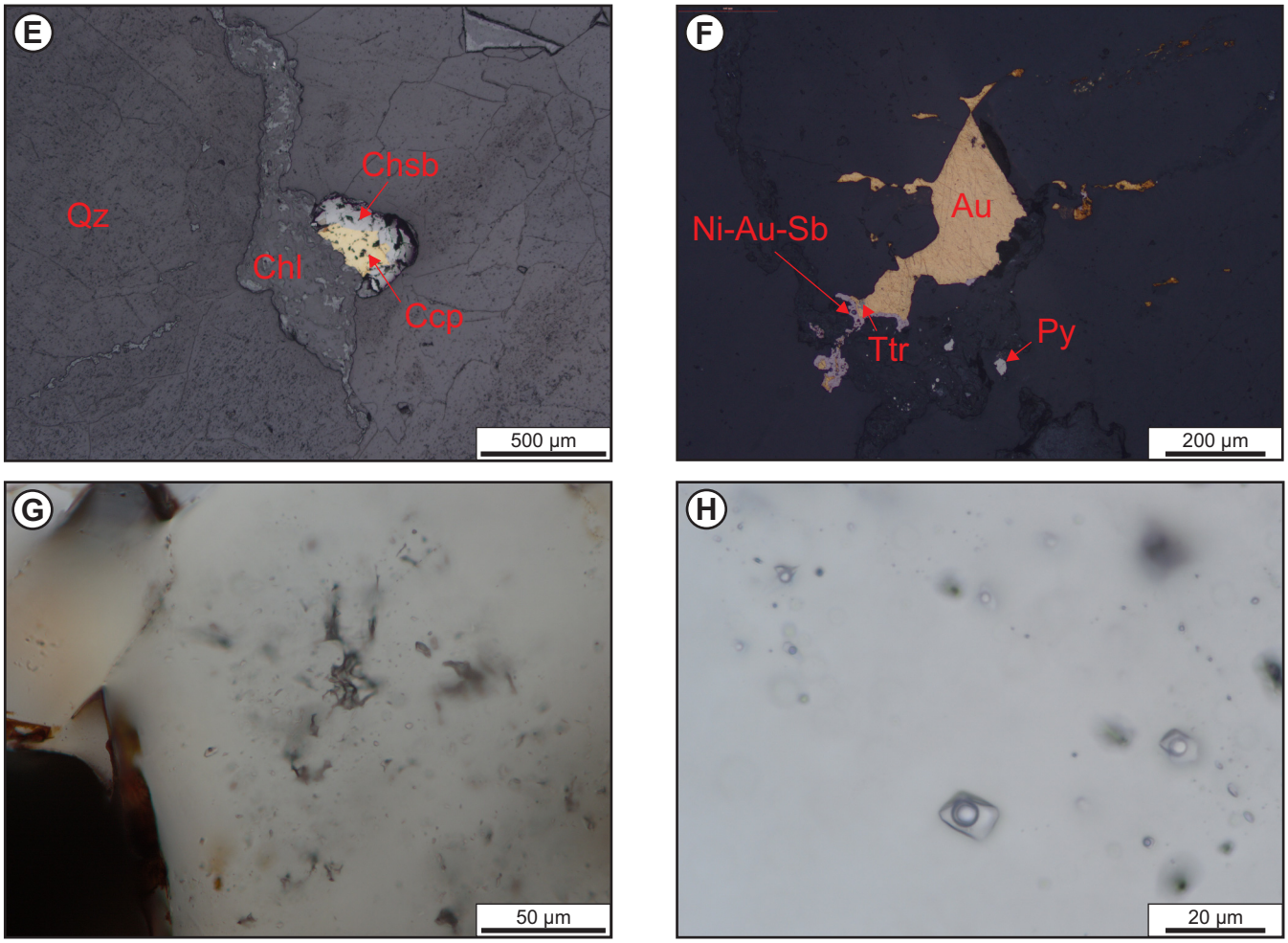

Plate 6 (Continued). *E) Stylolite in quartz vein, with chlorite and chalcopyrite rimmed by chalcostibite (sample 21HVB-412B, RL); F) Large gold grain with minor tetrahedrite and unknown Ni–Au–Sb mineral in quartz (sample 21HVB-421D, RL); G) Decrepitated fluid inclusion surrounded by small neonate inclusions (sample Dome 1, PPL); H) Three-phase aqueous carbonic inclusions in clear quartz associated with sulphide mineralization (sample Big Vein 2, PPL). All mineral abbreviations are from Whitney and Evans (2010).*

of indeterminate origin which did not show evidence of post-entrapment modification, and were spatially associated with mineralization, were identified in two samples, one from the Big Vein Depsoit and one from the Lotto Deposit (Table 2).

All fluid inclusions are three-phase aqueous-carbonic inclusions with proportions of the carbonic phase ranging from 20 to 40% (Plate 6H). T_m CO_2 ranges from -60.7 to -56.6°C, indicating compositions ranging from pure CO_2 to $CO_2$with minor amounts of other gases (*e.g.*, CH_4, N_2). The carbonic phase is low density and homogenizes to the vapour phase between 25 and 29.3°C. X_{CO2} ranges from 0.06 to 0.07 (Figure 2C), and clathrate melting between 7 and 8.5°C was used to calculate fluid salinities of 6.2 and 7.4 eq. wt. % NaCl. Total homogenization to the liquid was recorded in all inclusions between 233 and 313°C (Figure 2D). Isochore modelling using the spreadsheet of Steele-MacInnis (2018) indicate trapping pressures of 1.26 ± 0.09 kbars at 350°C and 2.80 ± 0.10 kbars at 500°C.

Sulphur-isotope Studies

Most samples contain no pyrite, thus data were collected from a single sample from the Keats Deposit of the Queensway Project. These grains are characterized by slightly negative $\delta^{34}S$ values, ranging from -0.4 ± 2.2 ‰ to -3.2 ± 1.7‰ (Table 3, Figure 3). Bulk sulphur-isotope data from prospects in the area of the Appleton Fault Zone were also reported by Evans and Wilson (1994) and O'Driscoll (2005) and fall within a similar range close to 0‰ (0.3 ± 0.4‰).

DISCUSSION

METAL ASSOCIATIONS AND ORE MINERALOGY

Metal associations and ore mineralogy vary greatly between gold occurrences in Newfoundland. The Cape Ray deposits are characterized by high base-metal contents and abundant chalcopyrite, galena and sphalerite associated with gold mineralization. In addition, the gold occurs in electrum grains with high silver contents (up to 46.7 wt. % Ag), and previous studies have identified significant bismuth in galena (up to 0.93 wt. % Bi; Wilton and Strong, 1986). Similarly, the prospects at Wilding Lake are locally enriched in copper, with Cu grades in Au-mineralized chalcopyrite-rich veins of up to 28.1%. These high base-metal contents are unusual for orogenic gold deposits (Goldfarb *et al.*, 2005) and may reflect leaching of metals from base-metal enriched source rocks or *via* atypical fluids (salinity, pH) during metamorphic devolatilization (Zhong *et al.*, 2015). Alternatively, these high base-metal contents may reflect a magmatic component, as was previously suggested for the Cape Ray Deposit by Wilton and Strong (1986).

The Valentine Lake deposits are characterized by relatively simple ore mineralogy, where pyrite is the only significant sulphide in association with gold mineralization and rare base-metal–telluride assemblages pre- or postdating the main gold mineralization event (Barrington *et al.*, 2016). Similarly, gold occurrences on Glover Island have only minor chalcopyrite and rare galena and Au–Ag–Pb sulphides and tellurides recorded in mineralized veins. At Moosehead, gold mineralization is associated with abundant sulphides and sulphosalts, including boulangerite, bournonite, pyrite, sphalerite, arsenopyrite, galena, chalcopyrite and chalcostibite, whereas gold deposits proximal to the Appleton Fault Zone are associated with abundant disseminated pyrite and arsenopyrite in the host rocks and minor pyrite, arsenopyrite, boulangerite, chalcostibite and chalcopyrite in the mineralized veins.

Numerous studies (Pitcairn *et al.*, 2006; Large *et al.*, 2011; Parnell *et al.*, 2017) have shown that for many orogenic gold deposits, the metal budget is controlled by reactions during greenschist- and amphibolite-facies metamorphism, particularly the transition from pyrite to pyrrhotite. However, some authors have suggested that enrichment in some elements (*e.g.*, Te) may instead represent a magmatic–hydrothermal input (*e.g.*, Spence-Jones *et al.*, 2018). If the metamorphic devolatilization model is accepted for gold mineralization in Newfoundland, the variations in ore mineralogy may reflect variations in the metal content of pyrite in the source rocks, but a possible magmatic source for some of these elements cannot be discounted for all deposits.

FLUIDS ASSOCIATED WITH GOLD MINERALIZATION

Fluid-inclusion studies in hydrothermal ore deposits require detailed petrographic analysis to identify the fluid responsible for the main mineralization event (as opposed to pre- or post-mineralizing fluid events), and for determining that the measured fluid composition represents the original, unmodified fluid composition of the mineralizing fluids (Roedder, 1984; Van den Kerkhof and Hein, 2001; Wilkinson, 2001; Bodnar, 2003; Goldstein, 2003; Chi *et al.*, 2020). This is particularly important in orogenic gold deposits, where gangue quartz commonly displays a complex history of ductile and brittle deformation, grain scale recrystallization and fluid inclusions show evidence for post entrapment modification such as decrepitation, leaking and stretching (Zoheir *et al.*, 2019; Tuba *et al.*, 2021; Tavares Nassif *et al.*, 2022). In addition, the overabundance and spatial superposition of fluid inclusions in some samples makes the determination of individual FIAs impossible (Zoheir *et al.*, 2019; Tuba *et al.*, 2021). These potential pitfalls were encountered in all samples analyzed during this study, with common decrepitation clusters (Plate 6G), evidence for plastic deformation (Plate 3G) and abundance of inclusions in gangue quartz (Plate 3F).

Despite these difficulties, primary FIAs along growth zones or FIAs of indeterminate origin in clear quartz associated with sulphide mineralization, without evidence of post-entrapment modification, were identified in 13 samples from five study areas (Table 2), and these fluids are interpreted to represent fluids associated with gold and sulphide mineralization. In all study areas, the mineralizing fluids were shown to be low-salinity, aqueous-carbonic fluids with minimum trapping temperatures of ~250–350°C (Figure 4). These fluids are typical of fluids associated with orogenic gold deposits (Ridley and Diamond, 2000; Bodnar *et al.*, 2014; Gaboury, 2019), and possible origins of these fluids is discussed by Goldfarb and Groves (2015). Although the fluid-inclusion data presented cannot unequivocally decipher the source of these aqueous-carbonic fluids in Newfoundland mineralization, most recent studies suggest that such fluids are related to metamorphic devolatilization of metasedimentary and mafic metavolcanic rocks at the greenschist-amphibolite transition (Phillips and Powell, 2010; Goldfarb and Pitcairn, 2023).

Along the mineralized fault zones, host rocks to the various occurrences in this study have undergone greenschist-facies metamorphism (Dubé *et al.*, 1996; Cawood and van Gool, 1998; Evans, 1999; Willner *et al.*, 2018), which would have facilitated the release of aqueous-carbonic fluids. However, Devonian regional metamorphism across the Dunnage Zone is lower grade with some Silurian rocks

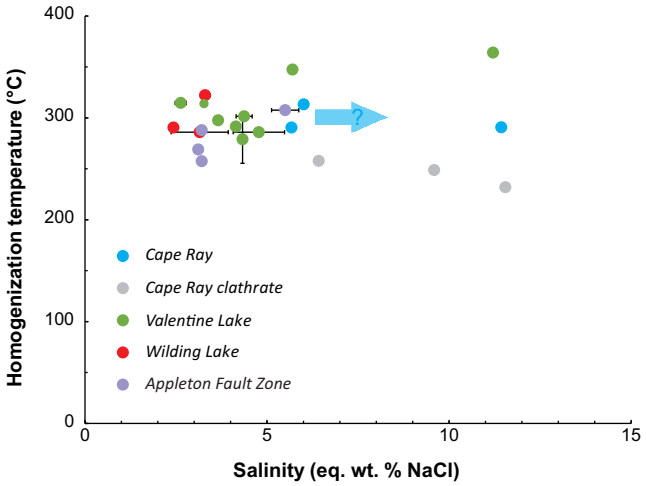

Figure 4. *Plot of fluid inclusion homogenization temperature* vs. *fluid salinity for aqueous-carbonic and aqueous-clathrate inclusions. Light blue arrow indicates possibly under estimation of fluid salinities in aqueous-carbonic inclusions at Cape Ray due to presence of* CH_4. See *text for details.*

unmetamorphosed and undeformed (*e.g.*, Honsberger *et al.*, 2022b). Fluid systems may have also been generated during Silurian (*ca.* 425–423 Ma; Dunning *et al.*, 1990; Buchannan and Bennett, 2009) exhumation and uplift of amphibolite-facies rocks within the Gander Zone, and/or during Devonian low-pressure/intermediate- to high-temperature contact metamorphism within the eastern Exploits Subzone (Currie and Pajari, 1981). Considering the widespread occurrence of felsic igneous rocks along the gold-mineralized belts of study, magmatic-derived fluid components produced *via* the degassing of felsic magmas cannot be discounted, as has been suggested by some authors as a possible source of aqueous-carbonic fluids in other orogenic gold deposits (*e.g.*, Hammond *et al.*, 2011; Treloar *et al.*, 2015; Spence-Jones *et al.*, 2018; Palinkaš *et al.*, 2024).

This study has identified significant variations in fluid composition and conditions of fluid precipitation between orogenic gold occurrences in central and southern Newfoundland. The low melting temperature of the carbonic phase at Cape Ray (down to -70°C; Figure 2A) illustrates that the mineralizing fluid contained significant amounts of dissolved gases other than CO_2 (*e.g.*, CH_4, N_2), which may reflect fluid-rock interaction within graphitic sediments of the Windsor Point Group resulting in a high-X_{CH4} (Tuba *et al.*, 2021). In addition, the presence of carbonic inclusions with no aqueous component and two-phase (liquid + vapour) aqueous inclusions in the same FIAs suggests fluid immiscibility was important in the formation of deposits at Cape Ray. Similar evidence for fluid immiscibility was also recorded during fluid-inclusion studies at the Moosehead Prospect (Conliffe and Wilton, 2009). No evidence for fluid immiscibility was recorded at Valentine Lake, Wilding Lake or along the Appleton Fault Zone.

Mineralizing fluids at Cape Ray have relatively high salinities when compared to other gold occurrences in central Newfoundland (Figure 4) and to fluids commonly associated with other orogenic gold systems globally (3–7 eq. wt. % NaCl; Ridley and Diamond, 2000; Goldfarb and Groves, 2015). The calculated fluid salinities for Cape Ray may be slightly underestimated because of the presence of CH_4 (Diamond, 1994). In orogenic gold systems, metals are thought to be transported predominantly as bisulphide complexes (Williams-Jones *et al.*, 2009), and the low concentrations of base metals in these systems is attributed to the low salinity of mineralizing fluids and the lack of chloride complexes to carry base metals (Phillips and Powell, 2010; Yardley and Cleverly, 2015). The higher salinities recorded from Cape Ray may indicate that mineralizing fluids were capable of moving base metals along fluid pathways and transporting metals in solution as chloride complexes (Yardley, 2005), resulting in the abundance of chalcopyrite, galena and sphalerite and the high Ag content of electrum at these deposits.

ESTIMATE OF DEPTHS OF MINERALIZATION

Fluid-inclusion data from aqueous-carbonic fluid inclusions were used to construct pressure-temperature isochores for mineralizing fluids (Figure 5), which can in turn be utilized to estimate the paleodepth of mineralization assuming an average rock density of 2.65 g/cm^3.

At Cape Ray, the average estimated fluid pressures from all FIAs range from ~2.77 to 3.71 kbars at 350°C and 4 to 5.88 kbars at 500°C, which correspond to depths of 10.7 to 14.3 km at 350°C and 15.4 to 22.3 km at 500°C. Paleodepths of >12 km are typical of hypozonal orogenic gold deposits in Archean terranes (Goldfarb *et al.*, 2005), but mineralization at Cape Ray occurred at lower temperatures than typical hypozonal orogenic gold deposits, under greenschist rather than amphibolite-facies conditions (Figure 5). However, *ca.* 417–400 Ma amphibolite-facies metamorphism occurs in the adjacent Gander Zone (van Staal *et al.*, 2024) and overlaps the proposed timing of deformation associated with orogenic gold mineralization (*ca.* 415–386 Ma; Dubé *et al.*, 1996; Sandeman *et al.*, 2022).

Estimated fluid pressures from the Valentine Lake deposits (2.42 ± 0.39 kbars at 350°C and 3.73 ± 0.62 kbars at 500°C) and Wilding Lake prospects (1.89 ± 0.34 kbars at 350°C and 2.90 ± 0.57 kbars at 500°C) correspond to paleodepths of ~7.3 to 14.3 km, which are typical of mesozonal

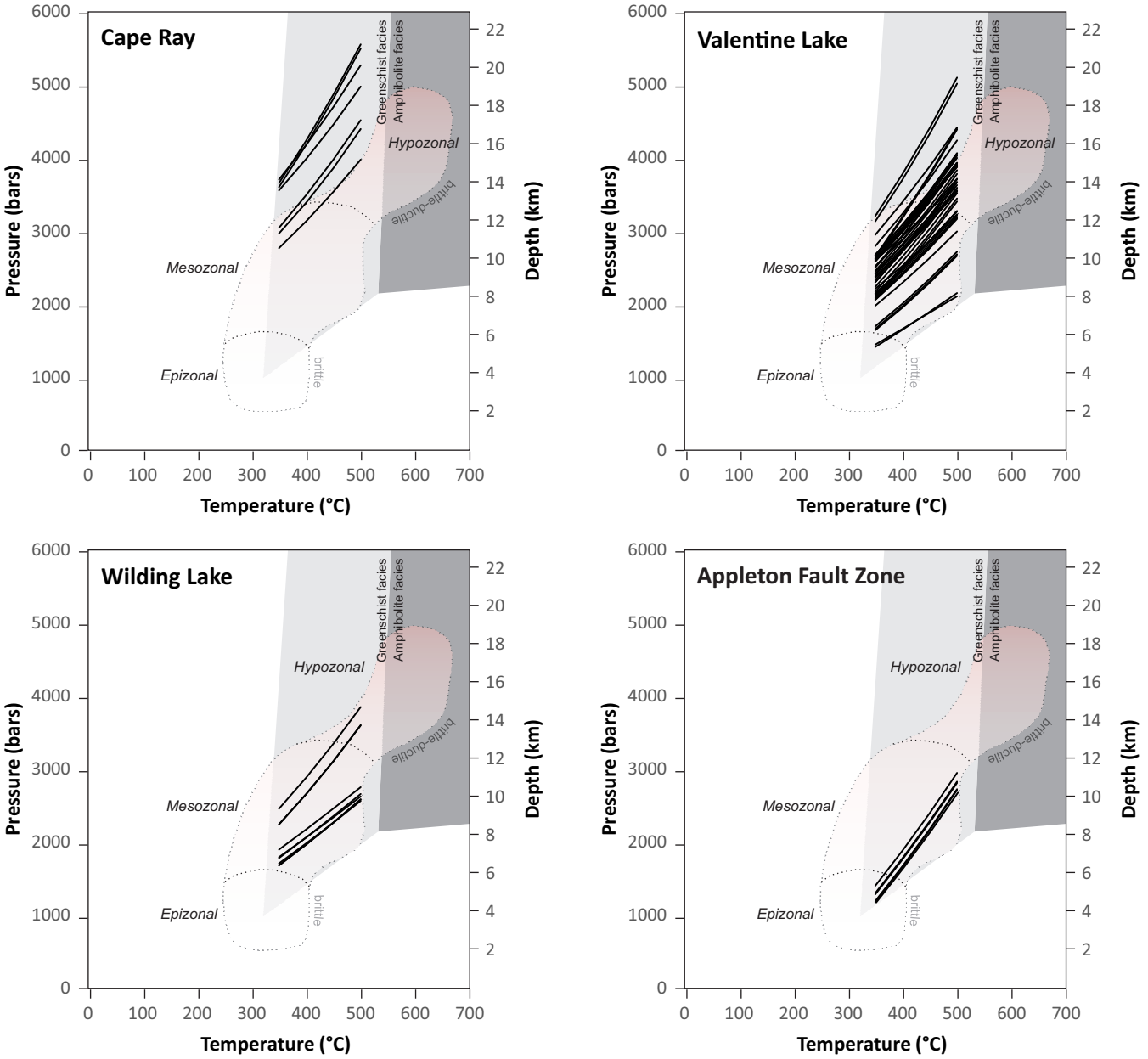

Figure 5. *Pressure temperature isochores for the Cape Ray, Valentine Lake, Wilding Lake and Appleton Fault Zone gold occurrences in central Newfoundland (adapted from Tuba* et al.*, 2021). Isochores reconstructing using microthermometric data from aqueous-carbonic fluid inclusions and using the spreadsheet of Steele-MacInnis (2018) for the H_2O- CO_2-NaCl system. Also included are metamorphic facies boundaries and typical P-T field for orogenic gold deposits (fields from Tuba* et al.*, 2021).*

orogenic gold deposits which form between 6 and 12 km depth (Figure 5; Goldfarb *et al.*, 2005).

Pressure estimates from the gold deposits at the Appleton Fault Zone range from 1.26 ± 0.09 kbars at 350°C and 2.80 ± 0.10 kbars at 500°C, corresponding to estimated paleodepths of 4.8 ± 0.3 km at 350°C and 10.8 ± 0.4 km at 500°C. Given the lower homogenization temperatures of fluid inclusions in these samples (Figure 2) it is likely that the lower paleodepth estimate is accurate, and gold deposits along the Appleton Fault Zone are epizonal gold deposits (formed at <6 km; Goldfarb *et al.*, 2005). This is consistent with petrographic evidence indicating that these occurrences formed at relatively shallow crustal levels, and are similar to previously published depth estimates from the Moosehead Prospect (~5.8 km; Conliffe and Wilton, 2009). Nearby antimony deposits that have zones enriched in gold (*e.g.*, Beaver Brook Antimony Deposit; Sandeman *et al.*, 2018) may also

have formed at shallow crustal levels during the same mineralization event. Similar textures and metal associations, with common breccia textures, abundant stylolites associated with gold mineralization and Sb enrichment have been reported from other shallow epizonal gold deposits globally with similar high gold grades (*e.g.*, Fosterville Deposit in Australia, Voisey *et al.*, 2020a),

Overall, these data indicate significant variations in the depths of mineralization that are preserved across central Newfoundland, with a general trend of shallower mineralization to the northeast. This trend reflects greater post-mineralization uplift/erosion in the southwest where protracted deformation occurred along the St. Lawrence Promontory, as evidenced by the narrowing of the Exploits Subzone from the northeast to southwest (Figure 1).

SULPHUR SOURCES

Sulphur isotope data from pyrite in orogenic gold occurrences of southern and central Newfoundland show a range of $\delta^{34}S$ values from close to 0‰ in the Appleton Fault Zone Deposits and at the Central Deposit at Cape Ray to ~10‰ at Valentine Lake; intra-deposit heterogeneity is variable (Table 3; Figure 3). These data fall within the ranges reported from other Phanerozoic orogenic gold deposits globally (Quesnel *et al.*, 2023), which have $\delta^{34}S$ values between -5 and 12‰, and a bimodal distribution with a main mode between 0 and 3‰ and a secondary mode at ~10‰ (Quesnel *et al.*, 2023; Figure 3). Variations in sulphur isotope values from sulphides in orogenic gold deposits have commonly been used to trace sulphur source(s) and have been attributed to variable inputs and mixing of magmatic- or mantle-derived sulphur or crustal sulphur leached from the surrounding host rocks (McCuaig and Kerrich, 1998; Goldfarb *et al.*, 2005). Alternatively, the wide range in $\delta^{34}S$ values recorded in individual orogenic gold deposits may be attributed to changes in the physiochemical conditions during gold precipitation (Palin and Xu, 2000; Herzog *et al.*, 2024). More recently, *in-situ* sulphur isotope analysis of pyrite in orogenic gold systems has identified significant heterogeneity in $\delta^{34}S$ values within individual pyrite grains. This has been attributed to mixing of multiple sulphur sources or fluid immiscibility leading to rapid changes in redox conditions (Bateman and Hagemann, 2004; Peterson and Mavrogenes, 2014; Ward *et al.*, 2017) which are highly sensitive to sulphur isotope fractionation between sulphate and sulphide (Ohmoto and Rye, 1979). Investigations of mass independent fractionation of sulphur (MIF-S) in Archean orogenic gold deposits have shown that wide variations in $\delta^{34}S$ values are attributable to variations of the oxidation state of the fluids regardless of the sulphur source (LaFlamme *et al.*, 2018; Petrella *et al.*, 2020; Sugiono *et al.*, 2022).

Previous sulphur isotope studies from central Newfoundland have identified intra-deposit variations in sulphur sources, with $\delta^{34}S$ values in pyrite close to 0‰ interpreted to represent magmatic sulphur sources (Wilton and Strong, 1986; Evans and Wilson, 1994; O'Driscoll, 2005; O'Driscoll and Wilton, 2005) and positive $\delta^{34}S$ values suggested to represent sulphur sourced from modified seawater sulphate (O'Driscoll, 2005). Data collected show sulphur isotope signatures that fall within similar ranges to these past studies, thus variations between occurrences may reflect sulphur sourced from different reservoirs. Sulphur isotope data from the Valentine Lake, Glover Island and Moosehead occurrences all show positive $\delta^{34}S$ values (Figure 3). These suggest that sulphur was derived from devolatilization of sedimentary hosted sulphur with a positive $\delta^{34}S$ signature during the pyrite–pyrrhotite transition (Pitcairn *et al.*, 2006) and is consistent with a metamorphic origin of mineralizing fluids. Data from the Cape Ray Central Deposit and deposits along the Appleton Fault Zone are close to 0‰, which may represent a magmatic sulphur source, either directly related to magmatism or *via* de-sulphidation of magmatic sulphides during metamorphism. At Cape Ray, the evidence for a magmatic fluid component may explain the high base-metal content of mineralized veins, but at mineralizing depths estimated in this study (>10 km) direct degassing of magmatic fluids is unlikely (Goldfarb and Pitcairn, 2023). In contrast, the low estimated emplacement depth for deposits along the Appleton Fault Zone (<6 km) could facilitate the direct degassing of magmatic fluids, and points to a direct magmatic–hydrothermal component of sulphur in this area.

In addition to variation in sulphur sources, the importance of physiochemical fluid changes such as redox reactions and fluid immiscibility must be considered to explain the intra- and inter-deposit heterogeneity in $\delta^{34}S$ values. Fluid inclusions studies have shown evidence for fluid immiscibility at Cape Ray and Moosehead, and rapid changes in fluid redox conditions during immiscibility may explain the heterogeneity of sulphur isotope systematics in pyrite grains (Sugiono *et al.*, 2022). The shift towards isotopically heavier $\delta^{34}S$ in the rims of pyrite grains from Glover Island may mark a shift to more reduced fluid conditions (H_2S dominated) during the later stages of mineralization which would have been capable of carrying gold in solution as $Au(HS)_2$ complexes (Williams-Jones *et al.*, 2009; Herzog *et al.*, 2024).

METALLOGENIC MODEL FOR GOLD MINERALIZATION IN SOUTHERN AND CENTRAL NEWFOUNDLAND

This study has shown that the studied gold occurrences can be broadly classified as orogenic as defined by Goldfarb

et al. (2005), and more specifically represent the crustal-scale fault-associated (CSF) sub-type of Phanerozoic orogenic gold deposits as defined by Mortenson *et al.* (2022). Gold mineralization is hosted in quartz–carbonate veins (rare, disseminated gold in surrounding host rock) that typically have laminated, ribbon or brecciated textures. The mineralizing fluids were low-salinity aqueous-carbonic fluids that likely carried gold in solution as bisulphide complexes, and locally show evidence of fluid unmixing and immiscibility related to rapid decompression (*e.g.*, Cape Ray, Moosehead). Mineralization occurred in an accretionary orogenic setting, with available geochronological data consistent with mineralization occurred in multiple cycles spanning the late stages of the Salinic as well as the Acadian and Neoacadian orogenic cycles (Sandeman *et al.*, 2022). There is a strong structural control on mineralization, with all occurrences related to intracontinental deformation along second and third order faults in proximity to crustal-scale transpressive fault zones (Dubé *et al.*, 1996; O'Brien, 2003; Honsberger *et al.*, 2019a). Mineralization occurs in a range of host rocks along these structures, indicating that structural setting and associated tectonic environment were the primary controls on gold deposition.

Despite these broad similarities and classification of all occurrences studied as CSF subtype orogenic gold deposits, there are significant variations between occurrences that are evident at the deposit scale and have important implications for exploration. These include variations in host rocks, metal associations and ore mineralogy, sulphur and fluid sources (as suggested by fluid inclusion and sulphur isotope data), and paleodepth of mineralization (hypozonal *vs.* mesozonal *vs.* epizonal). In addition, the depositional mechanism may have varied between deposits, with strong evidence for fluid immiscibility and changes in the physiochemical fluid conditions being responsible for gold precipitation at Cape Ray and Moosehead. Although no evidence for fluid immiscibility was recorded at other locations, the high abundance of decrepitation clusters in many samples, particularly from deposits at the Appleton Fault Zone, is indicative of hydrostatic pressure cycling in response to induced under- or overpressure (Tuba *et al.*, 2021), which could, in turn, have changed fluid compositions and facilitated gold precipitation. No evidence for fluid mixing was recorded so this is considered unlikely as a gold precipitation mechanism, and although wallrock sulphidation is not recorded in this study, it is a likely factor in the formation of other orogenic gold deposits in central Newfoundland (*e.g.*, Midway prospect, Honsberger *et al.*, 2023; Titan prospect, Squires, 2005; Duder Lake prospects, Churchill *et al.*, 1993). In addition, aseismic gold enrichment along pressure dissolution seams may be responsible for some of the high-grade gold mineralization at Moosehead and at deposits along the Appleton Fault Zone, similar to what has recently been described from the Fosterville Deposit (Voisey *et al.*, 2020b).

Sandeman *et al.* (2022) proposed two distinct intervals of gold mineralization across Newfoundland at *ca.* 433 to 405 Ma and at *ca.* 390 to 372 Ma, with hydrothermal rutile at Valentine Lake and Wilding Lake falling within the older time window and hydrothermal monazite and alteration muscovite from Valentine Lake falling within the younger interval. The other gold zones discussed have poorly constrained ages but probably fall within those broad intervals. During, and immediately prior to, the formation of gold mineralized zones across central and western Newfoundland, the lithosphere was extended to produce widespread Telychian to Lochkovian, non-arc bimodal gabbroic and granitic intrusions and volcanic equivalents of the Hodges Hill, Mount Peyton and Fogo Intrusive suites and correlative rocks in the Dunnage and Gander zones. Additional bimodal intrusive activity including the granodioritic Loon Bay pluton, granodiorite, monzonite and layered gabbros of the eastern Fogo Island Tilting complex, and the gabbroic Howley Island Intrusions occurred during the interval 408–400 Ma (Elliot *et al.*, 1991; Graham *et al.*, 2020; Honsberger *et al.*, 2024). This magmatic interval was, in turn, followed by the emplacement of numerous granitic intrusions within Ganderian basement across southern and east-central Newfoundland from *ca.* 395 to 378 Ma (Wang *et al.*, 2024).

Protracted emplacement of various igneous bodies presumably increased geothermal gradients in the crust significantly, generated metamorphic fluids *via* contact metamorphism at depth, and also may have increased and diversified granitophile metal budgets to the hydrothermal fluids. Therefore, although a metamorphic devolatilization model is likely the predominant source of mineralizing fluids, the close temporal and spatial link between the gold mineralization, regional deformation, and magmatism suggests that the polymetallic nature of some of the mineralized systems may result from magmatic fluid input.

CONCLUSIONS

This study provides detailed geological, petrographic, fluid-inclusion and sulphur isotope data from significant gold deposits and prospects in central and southern Newfoundland, an emerging gold district that has not been the subject of extensive previous published geological study. Mineralization typically occurs in quartz–carbonate veins, with highly variable ore mineralogy and metal associations ranging from base-metal rich (*e.g.*, Cape Ray deposits) to base-metal poor (*e.g.,* Valentine Lake deposits). All occurrences show a close spatial association with major faults and

are hosted in a wide range of rocks along generally low-grade deformation corridors that locally retain greenschist-facies alteration assemblages. Fluid-inclusion analysis shows that mineralizing fluids are low-salinity, aqueous-carbonic fluids, and mineralization occurred at a wide range of paleodepths, ranging from relatively deep mesozonal mineralization (>10 km) to shallow epizonal mineralization (<6 km). Sulphur-isotope analysis of pyrite indicates variations in sulphur sources between study areas, with positive $\delta^{34}S$ values indicative of sulphur sourced during metamorphic devolatilization and $\delta^{34}S$ values close to 0‰ indicating a magmatic sulphur source. In addition, intra-deposit variations in $\delta^{34}S$ values of pyrite may reflect physiochemical fluid changes during gold mineralization.

Based on their geological characteristics, these occurrences have been classified as crustal-scale fault-associated subtype of orogenic gold deposits as defined by Mortenson *et al.* (2022). Gold mineralization occurred during post-Salinic extension and spanned the Acadian and Neoacadian orogenic cycles, with mineralizing fluids likely generated at multiple times from devolatilization reactions associated with metamorphism. However, sulphur isotope data suggest a magmatic–hydrothermal component in some occurrences, and the close spatial and temporal association of gold mineralization with voluminous granitoid bodies suggest that these may be important to the formation of some orogenic gold systems in Newfoundland.

The results here have important implications for gold exploration in Newfoundland, showing that second and third order faults within low-grade structural domains that preserve local greenschist-facies metamorphism adjacent to higher grade belts (*e.g.*, External Humber Zone and Gander Zone) are the best targets for future exploration. The variations in metal associations outlined in this study should be accounted for when determining suitable geochemical vectors used in in regional exploration programs. Future work should aim to better understand the deposit-scale processes associated with the formation of orogenic gold mineralization in Newfoundland, including detailed trace-element and sulphur isotope mapping of sulphides associated with gold mineralization, and further analysis of fluids associated with gold mineralization.

ACKNOWLEDGMENTS

Many thanks to Aumega Metals, Calibre Mining, Labrador Gold Corporation, New Found Gold Corporation and Sokoman Minerals Corporation for providing access and samples from gold deposits. JC and HS thank their colleagues at the Geological Survey of Newfoundland and Labrador for assistance during multiple field seasons, particularly the hard work and dedication of summer students David Drover, Erin Butler, Maria O'Neill and Taylor Mugford. John Hinchey provided a detailed and thoughtful review of an earlier version of this manuscript. The technical support of Dylan Goudie and Glenn Piercey (Memorial University) during collection of SEM-MLA and fluid-inclusion data was greatly appreciated. Sulphur isotope data was acquired with the assistance of Guillaume Barré (Université Laval, currently Geological Survey of Canada). IWH acknowledges funding from NRCan's Targeted Geoscience Initiative 6 and thanks Matt Polivchuk for SEM data acquisition.

REFERENCES

Bakker, R.J.
1997: CLATHRATES: computer programs to calculate fluid inclusion V-X properties using clathrate melting temperatures. Computer Geoscience, Volume 23, pages 1-18.

2003: Package FLUIDS 1. Computer programs for analysis of fluid inclusion data and for modelling bulk fluid properties. Chemical Geology, Volume 194, pages 3-23.

Barbour, D.M.
2004: Tenth year supplementary assessment report on diamond drilling exploration for license 9856M on claims in the Bishops Falls area, central Newfoundland. Newfoundland and Labrador Geological Survey, Assessment File NFLD/2890, 55 pages.

Barbour, D., Regular, M., Ewert, W. and Puritch, E.J.
2012: Assessment report on compilation, resource estimation and diamond drilling exploration for 2012 submission for mining lease 190 and for fourth and twelfth year assessment for licences 7584M and 15583M on claims in the Glover Island area, western Newfoundland, 3 reports. Mountain Lake Minerals Incorporated, Newfoundland and Labrador Geological Survey, Assessment File 12A/1622, 724 pages.

Barre, G. and LaFlamme, C.
2023: Delineating the sulfur isotope signature of a VMS district by LA-ICP-QQQ-MS. Society of Geology Applied to Mineral Deposits, proceedings of the 17th SGA Biennial Meeting, Zurich, Switzerland, pages 240-243.

Barrington, M.A., Layne, G.D., Dunning, G.R. and Dunsworth, S.
2016: A mineralogical, geochemical, and geochronological study of Marathon Gold Corporation's Valentine Lake Gold Camp, central Dunnage Zone, Newfound-

land, Canada. Geological Association of Canada Newfoundland and Labrador Section, 2016 Spring Technical Meeting, Abstract, 1 page.

Bateman, R. and Hagemann, S.
2004: Gold mineralisation throughout about 45 Ma of Archaean orogenesis: Protracted flux of gold in the Golden Mile, Yilgarn craton, Western Australia. Mineralium Deposita, Volume 39, pages 536-559.

Blackwood, R.F.
1982: Gander (Mount Peyton E.), Newfoundland, Map 80-198, scale: 1:50 000. *In* Geology of the Gander Lake (2D/15) and Gander River (2E/2) Area. Government of Newfoundland and Labrador, Department of Mines and Energy, Mineral Development Division, Report 82-04, 63 pages.

Bodnar R.J.
2003: Re-equilibration of fluid inclusions. *In* Fluid Inclusions: Analysis and Interpretation. *Edited by* I. Samson, A. Anderson and D. Marshall. Mineralogical Association of Canada, Short Course 32, pages 213-230.

Bodnar, R.J., Lecumberri-Sanchez, P., Moncada, D. and Steele-MacInnis, M.
2014: Fluid inclusions in hydrothermal ore deposits. *In* Treatise on Geochemistry, 2nd Edition. *Edited by* H.D. Holland and K.K. Turekian. Elsevier, Oxford/San Diego, pages 119-142.

Boyce, W.D., Ash J.S. and O'Brien B.H.
1991: A new fossil locality in the Bay of Exploits, central Newfoundland. *In* Current Research. Government of Newfoundland and Labrador, Department of Mines and Energy, Geological Survey Branch, Report 91-1, pages 79-82.

Brem, A.G.
2007: The Late Proterozoic to Palaeozoic Tectonic Evolution of the Long Range Mountains in Southwestern Newfoundland. Unpublished Ph.D. thesis, University of Waterloo, Waterloo, ON, Canada, 178 pages.

Castonguay, S., Skulski, T., van Staal, C. and Currie, M.
2009: New insights on the structural geology of the Pacquet Harbour Group and Point Rousse Complex, Baie Verte Peninsula. *In* Current Research. Government of Newfoundland and Labrador, Department of Natural Resources, Geological Survey, Report 091, pages 147-158.

Cawood, P.A. and van Gool, J.A.M.
1998: Geology of the Corner Brook–Glover Island Region, Newfoundland. Geological Survey of Canada, Bulletin 427, 96 pages.

Chandler, F.W., Loveridge, D. and Currie, K.L.
1987: The age of the Springdale Group, western Newfoundland, and correlative rocks - evidence for a Llandovery overlap assemblage in the Canadian Appalachians. Transactions of the Royal Society of Edinburgh: Earth Science, Volume 78, pages 41-49.

Chi G-X, Diamond LW, Lu H-Z, Lai J-Q and Chu H-X
2020: Common problems and pitfalls in fluid inclusion study: A review and discussion. Minerals, Volume 11. https://doi.org/10.3390/min11010007

Churchill, R.A., Wilton, D.H.C. and Evans, D.T.W.
1993: Geology, alteration assemblages and geochemistry of the Duder Lake gold showings, northeastern Newfoundland. *In* Current Research. Government of Newfoundland and Labrador, Department of Mines and Energy, Geological Survey Branch, Report 93-1, pages 317-333.

Colman-Sadd, S., Hayes, J. and Knight, I.
1990: The Geology of the Island of Newfoundland. Map 90-01, Scale 1:1 000 000. Government of Newfoundland and Labrador, Department of Mines and Energy, Geological Survey Branch, Geofile Number NFLD/2192.

Conliffe, J. and Wilton, D.H.C.
2009: Fluid inclusion studies of mineralized and barren quartz veins associated with gold mineralization at the Moosehead Property, central Newfoundland. Government of Newfoundland and Labrador, Department of Natural Resources, Geological Survey, Internal Collection Report, Geofile Number NFLD/3469, 24 pages.

Conliffe, J.
2021: Structurally controlled orogenic gold mineralization in the Glover Island and Grand Lake area, western Newfoundland. *In* Current Research. Government of Newfoundland and Labrador, Department of Natural Resources, Geological Survey, Report 21-1, pages 1-26.

2022: VMS-style mineralization in the Kettle Pond Formation, Glover Island (NTS map areas 12A/12 and 13). *In* Current Research. Government of Newfoundland and Labrador, Department of Industry, Energy, and Technology, Geological Survey, Report 22-1, pages 1-27.

Coyle, M. and Strong, D.F.
1987: Geology of the Springdale Group: A newly recognized Silurian epicontinental-type caldera in Newfoundland. Canadian Journal of Earth Sciences, Volume 24(6), pages 1135-1148.

Currie, K.L. and Pajari, G.E.
1981: Anatectic peraluminous granites from the Carmanville area, northeastern Newfoundland. Canadian Mineralogist, Volume 19, pages 147-161.

Diamond, L.W.
1994: Salinity of multivolatile fluid inclusions determined from clathrate hydrate stability. Geochimica et Cosmochimica Acta, Volume 58, pages 19-41.

Dickson, W.L., O'Brien, B.H. and Colman-Sadd, S.P.
2000: Geology of the Botwood map area (NTS 2E/3), central Newfoundland. Map 2000-11, Scale 1:50 000. Government of Newfoundland and Labrador, Department of Mines and Energy, Geological Survey, Open File 2E/03/1067 Version 2.0.

Dubé, B., Dunning, G.R., Lauziere, K. and Roddick, J.C.
1996: New insights into the Appalachian Orogen from geology and geochronology along the Cape Ray fault zone, southwest Newfoundland. Geological Society of America Bulletin, Volume 108, pages 101-116. https://doi.org/10.1130/0016-7606(1996)108<0101:NIITAO>2.3.CO;2

Dubé, B. and Gosselin, P.
2007: Greenstone-hosted quartz-carbonate vein deposits. *In* Mineral Deposits of Canada: A Synthesis of Major Deposit Types, District Metallogeny, the Evolution of Geological Provinces, and Exploration Methods. *Edited by* W.D. Goodfellow. Geological Association of Canada, Mineral Deposits Division, Special Publication No. 5, pages 49-73.

Dubé, B. and Lauzière, K.
1997: Gold metallogeny of the Cape Ray fault zone, southwest Newfoundland: Geological Survey of Canada, Bulletin 508, 90 pages.
https://doi.org/10.4095/209256

Dunning, G., O'Brien, S.J., Colman-Sadd, S.P., Blackwood, R.F., Dickson, W.L., O'Neill, P.P. and Krogh, T.E.
1990: Silurian orogeny in the Newfoundland Appalachians. The Journal of Geology, Volume 98, pages 895-913.

Eccles, D.R., Jorgensen. M.K. and Simmons, G.
2024: New Found Gold Corp's Queensway Gold Project in Newfoundland and Labrador, Canada: 2024 Exploration Update. NI-43-101 technical report for New Found Gold Corp by APEX Geoscience Ltd., Jorgensen Engineering and Technical Services and GL Simmons Consulting, 326 pages.

Elliott, C.G., Dunning, G.R. and Williams, P.F.
1991: New U/Pb zircon age constraints on the timing of deformation in north-central Newfoundland and implications for early Paleozoic Appalachian orogenesis. Geological Society of America Bulletin, Volume 103, pages 125-135.
https://doi.org/10.1130/0016-7606(1991)103<0125:NUPZ AC>2 .3.CO;2.

Evans, D.T.W.
1996: Epigenetic gold occurrences, eastern and central Dunnage Zone, Newfoundland: Government of Newfoundland and Labrador, Department of Mines and Energy, Geological Survey, Mineral Resources Report 9, 135 pages.

1999: Epigenetic gold mineralization, Baie Verte Peninsula, Newfoundland. *In* Current Research. Government of Newfoundland and Labrador, Department of Mines and Energy, Geological Survey, Report 99-1, pages 163-182.

2020: NI 43-101 Technical Report on the Wilding Lake Project Central Newfoundland, Canada. NI-43-101 technical report for Canterra Minerals Corporation by Pendragon Consulting, 143 pages.

Evans, D.T.W. and Kean, B.F.
2002: The Victoria Lake Supergroup, central Newfoundland - Its definition, setting and volcanogenic massive sulphides mineralization. Government of Newfoundland and Labrador, Department of Mines and Energy, Geological Survey, Open File NFLD/2790, 80 pages.

Evans, D.T.W., Kean, B.F. and Dunning, G.R.
1990: Geological studies, Victoria Lake Group, central Newfoundland. *In* Current Research. Government of Newfoundland and Labrador, Department of Mines and Energy, Geological Survey Branch, Report 90-1, pages 135-144.

Evans, D.T.W. and Wilson, M.
1994: Epigenetic gold occurrences in the eastern Dunnage Zone, Newfoundland: Preliminary stable-isotope results. *In* Current Research. Government of Newfoundland and Labrador, Department of Mines and Energy, Geological Survey Branch, Report 94-1, pages 211-223.

Frimmel, H.E.
2008: Earth's continental crustal gold endowment. Earth and Planetary Science Letters, Volume 267, pages 45-55.

Gaboury, D.
2019: Parameters for the formation of orogenic gold deposits. Applied Earth Science, Volume 128, pages 124-133
https://doi.org/10.1080/25726838.2019.1583310

Goldfarb, R.J., Baker, T., Dubé, B., Groves, D.I., Hart, C.J.R. and Gosselin P.
2005: Distribution, character, and genesis of gold deposits in metamorphic belts. *In* Economic Geology 100th Anniversary Volume. *Edited by* J.W. Hedenquist, J.F.H. Thompson, R.J. Goldfarb and J.P. Richards. Society of Economic Geologists, pages 407-450.

Goldfarb, R.J. and Groves, D.I.
2015: Orogenic gold: Common or evolving fluid and metal sources through time. Lithos, Volume 233, pages 2-26.

Goldfarb, R.J. and Pitcairn I.
2023: Orogenic gold: Is a genetic association with magmatism realistic? Mineralium Deposita, Volume 58, pages 5-35.

Goldstein R.H.
2003: Petrographic analysis of fluid inclusions. *In* Fluid Inclusions: Analysis and Interpretation. *Edited by* I. Samson, A. Anderson, D. Marshall. Mineralogical Association of Canada, Short Course Series 32, pages 9-54.

Goldstein R.H. and Reynolds T.J.
1994: Systematics of fluid inclusions in diagenetic minerals. SEPM Short Course Notes, Volume 31, 188 pages.

Graham, B., Dunning, G. and Leitch, A.M.
2020: Magma mushes of the Fogo Island batholith: a study of magmatic processes at multiple scales. Journal of Petrology, Volume 61(10), pages 1-23.
https://doi.org /10.1093/petrology/egaa097.

Groves, D.I., Goldfarb, R.J., Gebre-Mariam, M., Hagemann, S.G. and Robert F.
1998: Orogenic gold deposits: A proposed classification in the context of their crustal distribution and relationship to other gold deposit types. Ore Geology Reviews, Volume 13, pages 7-27.

Groves, D.I., Goldfarb, R.J., Robert, F. and Hart, C.J.R.
2003: Gold deposits in metamorphic belts: Overview of current understanding, outstanding problems, future research, and exploration significance. Economic Geology, Volume 98, pages 1-29.

Hammond, N.Q., Robb, L.J., Foya, S. and Ishiyama, D.
2011: Mineralogical, fluid inclusion and stable isotope characteristics of Birimian orogenic gold mineralization at the Morila Mine, Mali, West Africa. Ore Geology Reviews, Volume 39, pages 218-229.

Herzog, M., LaFlamme, C., Beaudoin, G., Barré, G., Martin, L. and Savard, D.
2024: Fluid-rock sulfidation reactions control Au-Ag-Te-Bi precipitation in the Val-d'Or orogenic gold vein field (Abitibi subprovince, Canada). Mineralium Deposita, Volume 59, pages 1039-1064.
https://doi.org/10.1007/s00126-024-01247-6

Honsberger, I.W., Bleeker, W., Kamo, S.L., Sandeman, H.A.I., Evans, D.T.W., Rogers, N., van Staal, C.R. and Dunning, G.R.
2022a: Latest Silurian syntectonic sedimentation and magmatism and Early Devonian orogenic gold mineralization, central Newfoundland Appalachians, Canada: Setting, structure, lithogeochemistry, and high-precision U–Pb geochronology. Geological Society of America Bulletin.
https://doi.org/10.1130/GSAB.S.18858221.v1

Honsberger, I.W., Bleeker, W., Sandeman, H.A.I. and Evans, D.T.W.
2019a: Lithological and structural setting of structurally controlled gold mineralization in the Wilding Lake region, central Newfoundland. *In* Targeted Geoscience Initiative, 2018 report of activities. *Edited by* N. Rogers. Geological Survey of Canada, Open File 8549, pages 59-69. https://doi.org/10.4095/313640

2019b: Structural geology of a gold-bearing quartz vein system, Wilding Lake region, central Newfoundland. *In* Current Research. Government of Newfoundland and Labrador, Department of Natural Resources, Geological Survey, Report 19-1, pages 23-38.

Honsberger, I.W., Sandeman, H.A.I., Bleeker, W. and Kamo, S.L.
2023: Gabbro intrusions along the Dog Bay Line–Appleton Fault Zone gold corridor, northeast-central Newfoundland: U–Pb baddeleyite geochronology and lithogeochemistry. *In* Current Research. Government of Newfoundland and Labrador, Department of Industry,

Energy and Technology, Geological Survey, Report 23-1, pages 31-46.

Honsberger, I.W., Sandeman, H.A.I., Kamo, S.L. and Bleeker, W.
2024: Petrogenesis and high-precision U-Pb zircon geochronology of the Howley Islands intrusions, central Newfoundland Appalachians: Hydrous magmatism of Emsian age (*ca.* 400 Ma) along a multi-million ounce orogenic gold belt. Lithos, Volume 488-489. https://doi.org/10.1016/j.lithos.2024.107837

Honsberger, I.W., Wouter, B., Kamo, S.L., Sutcliffe, C.N. and Sandeman, H.A.I.
2022b: U–Pb geochronology of Late Silurian (Wenlock to Pridoli) volcanic and sedimentary rocks, central Newfoundland Appalachians: Targeting the timing of transient extension as a prelude to Devonian orogenic gold mineralization. Atlantic Geoscience, Volume 58, pages 215-237. https://doi.org/10.4138/atlgeo.2022.009

Kellett, D.A., Warren, C., Larson, K.P., Zwingmann, H., van Staal, C.R. and Rogers, N.
2016: Influence of deformation and fluids on Ar retention in white mica: Dating the Dover Fault, Newfoundland Appalachians. Lithos, Volume 254-255, pages 1-17.

LaFlamme, C., Martin, L., Jeon, H., Reddy, S.M., Selvaraja, V., Caruso, S., Bui, T-H., Roberts, M.P., Voute, F., Hagemann, S., Wacey, W., Littman, S., Wing, B., Fiorentini, M. and Kilburn, M.R.
2016: *In situ* multiple sulfur isotope analysis by SIMS of pyrite, chalcopyrite, pyrrhotite, and pentlandite to refine magmatic ore genetic models. Chemical Geology, Volume 444, pages 1-15. https://doi.org/10.1016/j.chemgeo.2016.09.032

LaFlamme. C., Sugiono, D., Thébaud, N., Caruso, S., Fiorentini, M., Selvaraja, V., Jeon H., Voute, F. and Martin, L.
2018. Multiple sulfur isotopes monitor fluid evolution of an Archean orogenic gold deposit. Geochimica et Cosmochimica Acta, Volume 222, pages 436-446.

Landry, P., Engelbrecht, L., Robson, D.M. and Smith, S.H.
2025: NI 43-101 Technical Report for the Queensway Gold Project, Newfoundland and Labrador, Canada. NI-43-101 technical report for New Found Gold Corp by SLR Consulting (Canada) Ltd. and Stantec Consulting Limited, 352 pages.

Large R.R., Bull S.W. and Maslennikov V.V.
2011: A carbonaceous sedimentary source-rock model for Carlin-type and orogenic gold deposits. Economic Geology, Volume 106, pages 331-358.

Layne, G.D., Barrington, M., Samson, C. and Capps, N.J.M.
2023: The Valentine Gold Project: Paleozoic Orogenic Gold Deposition in the Central Newfoundland Gold Belt. GAC-MAC-SGA 2023 Sudbury Meeting: Abstracts, Geoscience Canada, Volume 50, pages 1-4.

Mănuc, G.
2023: Structural controls on multistage gold mineralisation within the Baie Verte Peninsula of Newfoundland, Canada. Unpublished Ph.D. thesis, The University of Leeds, Leeds, UK, 538 pages.

McCuaig, T.C. and Kerrich R.
1998: P-T-t deformation-fluid characteristics of lode gold deposits: Evidence from alteration systematics. Ore Geology Reviews, Volume 12, pages 381-453.

McNicoll, V.J., Squires, G.C., Wardle, R.J., Dunning, G.R. and O'Brien, B.H.
2006: U–Pb geochronological evidence for Devonian deformation and gold mineralization in the eastern Dunnage Zone, Newfoundland. *In* Current Research. Government of Newfoundland and Labrador, Department of Natural Resources, Geological Survey, Report 06-1, pages 45-60.

Morgan, J.
2016: First year assessment report on geological, geochemical and trenching exploration for licences 22789M-22800M and 23582M-23587M on claims in the Bishops Falls area, central Newfoundland. Newfoundland and Labrador Geological Survey, Assessment File NFLD/3360, 317 pages.

Mortensen, J.K., Craw, D. and MacKenzie, D.J.
2022: Concepts and revised models for Phanerozoic orogenic gold deposits. *In* Recent Advances in Understanding Gold Deposits: From Orogeny to Alluvium. *Edited by* T.M. Torvela, R.J. Chapman and J. Lambert-Smith. Geological Society of London, Special Publication, Volume 516, pages 15-46.

Neuman, R.B.
1967: Bedrock geology of the Shin Pond and Stacyville Quadrangles Penobscot County, Maine. United States Department of the Interior, Geological Survey, Professional Paper 524-I, 50 pages.

O'Brien, B.H.
2003: Geology of the central Notre Dame Bay region (parts of NTS areas 2E/3, 6, 11), northeastern

Newfoundland. Government of Newfoundland and Labrador, Department of Mines and Energy, Geological Survey, Report 03-03, 147 pages.

O'Brien, B.H., O'Brien, S.J. and Dunning, G.R.
1991: Silurian cover, late Precambrian–Early Ordovician basement, and the chronology of Silurian orogenesis in the Hermitage Flexure (Newfoundland Appalachians). American Journal of Science, Volume 291, pages 760-799. https://doi.org/10.2475/ajs.291.8.760

O'Driscoll, J.M.
2005: An integrated geological, geochemical, isotopic and geochronological study on the auriferous systems in the Botwood Basin and environs, central Newfoundland. Unpublished M.Sc. thesis, Memorial University of Newfoundland, 456 pages.

O'Driscoll, J.M. and Wilton, D.H.C
2005: Preliminary geochronological, geochemical and isotopic studies of auriferous systems in the Botwood Basin and environs, central Newfoundland. *In* Current Research. Government of Newfoundland and Labrador, Department of Natural Resources, Geological Survey, Report 05-1, pages 207-222.

Ohmoto, H. and Rye, R.O.
1979: Isotopes of sulfur and carbon. *In* Geochemistry of Hydrothermal Ore Deposits. *Edited by* H.L. Barnes. John Wiley & Sons, New York, pages 509-567.

O'Neill, P.
1991: Geology of the Weir's Pond area, Newfoundland (NTS 2E/1). Government of Newfoundland and Labrador, Department of Mines and Energy, Geological Survey Branch, Report 91-03, 164 pages.

O'Neill, P. and Knight, I.
1988: Geology of the east half of the Weir's Pond (2E/1) map area and its regional significance. *In* Current Research. Government of Newfoundland and Labrador, Department of Mines, Mineral Development Division, Report 88-1, pages 165-176.

Palin, J.M. and Xu, Y.
2000: Gilt by association? Origins of pyritic gold ores in the Victory mesothermal gold deposit, Western Australia. Economic Geology, Volume 95, pages 1627-1634.

Palinkaš, S.S., Forsberg, F.R., Pedersen, R.B., Stubseid, H.H., McClenaghan, S.H. and Spangenberg, J.E.
2024: Metallogenic model of the Lykling ophiolite-hosted lode Au deposit, Scandinavian Caledonides: Insight from fluid inclusions, mineral chemistry and stable isotope geochemistry. Ore Geology Reviews, Volume 173.
https://doi.org/10.1016/j.oregeorev.2024.106227

Parnell, J., Perez, M., Armstrong, J., Bullock, L., Feldmann J. and Boyce, A.J.
2017: A black shale protolith for gold-tellurium mineralization in the Dalradian Supergroup (Neoproterozoic) of Britain and Ireland. Applied Earth Science, Volume 126, pages 161-175.

Peterson, E.C. and Mavrogenes, J.A.
2014: Linking high-grade gold mineralization to earthquake-induced fault-valve processes in the Porgera gold deposit, Papua New Guinea. Geology, Volume 42, pages 383-386.

Petrella, L., Thébaud, N., LaFlamme, C., Martin, L., Occhipinti, S. and Bigelow, J.
2020: *In-situ* sulfur isotopes analysis as an exploration tool for orogenic gold mineralization in the Granites-Tanami Gold Province, Australia: Learnings from the Callie deposit. Journal of Geochemical Exploration, Volume 214, Article 106542.
https://doi.org/10.1016/j.gexplo.2020.106542

Phillips, G.N. and Powell, R.
2010: Formation of gold deposits: A metamorphic devolatilization model. Journal of Metamorphic Geology, Volume 28, pages 689-718.

Pitcairn I.K., Craw D. and Teagle, D.A.H.
2015: Metabasalts as sources of metals in orogenic gold deposits. Mineralium Deposita, Volume 50, pages 373-390.

Pitcairn I.K., Teagle, D.A.H., Craw, D., Olivo, G.R., Kerrich, R. and Brewer T.S.
2006: Sources of metals and fluids in orogenic gold deposits: Insights from the Otago and Alpine schists, New Zealand. Economic Geology, Volume 101, pages 1525-1546.

Powell, J., Smith, S., Schulte, M., Merry, P.H., Russell, S., Anstey-Moore, C., Haghighi, B., Goode, J.R., Lipiec, I.A., Hernandez, S. and Raponi, T.R.
2022: Valentine Gold Project NI 43-101 technical report and feasibility study, Newfoundland and Labrador, Canada. NI-43-101 technical report by Marathon Gold Corporation, 536 pages.

Puritch, E. and Barry, J.
2017: Technical report and resource estimate on the Glover Island Gold Property, Grand Lake area west-central Newfoundland, Canada. NI-43-101 & 43-101F1 technical report for Mountain Lake Minerals Inc. by P&E Mining Consultants Inc., 118 pages.

Quesnel, B., Scheffer, C. and Beaudoin, G.
2023: The light stable isotope (hydrogen, boron, carbon, Nitrogen, oxygen, silicon, sulfur) composition of orogenic gold deposits. *In* Isotopes in Economic Geology, Metallogenesis and Exploration. *Edited by* D. Huston and J. Gutzmer. Mineral Resource Reviews, Springer Nature, pages 283-328.
https://doi.org/10.1007/978-3-031-27897-6_10

Ramezani, J., Dunning, G.R. and Wilson, M.R.
2000: Geologic setting, geochemistry of alteration, and U-Pb age of hydrothermal zircon from the Silurian Stog'er Tight. Gold Prospect, Newfoundland Appalachians, Canada. Exploration and Mining Geology, Volume 9, pages 171-188.

Ridley, J.R. and Diamond, L.W.
2000: Fluid chemistry of orogenic lode gold deposits and implications for genetic models. Reviews in Economic Geology, Volume 13, pages 141-162.

Roedder, E.
1984: Fluid Inclusions. Reviews in Mineralogy, Volume 12. Mineralogical Society of America, Washington, DC, 646 pages.

Rogers, N. and van Staal, C.
2002: Toward a Victoria Lake Supergroup: a provisional stratigraphic revision of the Red Indian to Victoria lakes area, central Newfoundland. *In* Current Research. Government of Newfoundland and Labrador, Department of Mines and Energy, Geological Survey, Report 02-1, pages 185-195.

Rogers, N., van Staal, C.R., McNicoll, V.J., Pollock, J., Zagorevski, A. and Whalen, J.
2006: Neoproterozoic and Cambrian arc magmatism along the eastern margin of the Victoria Lake Supergroup: A remnant of Ganderian basement in central Newfoundland? Precambrian Research, Volume 147, pages 320-341.
https://doi.org/10.1016/j.precamres.2006.01.025

Sandeman, H.A.I., Dunning, G.R., McCullough, C.K. and Peddle, C.
2017: U–Pb geochronology, petrogenetic relationships and intrusion-related precious-metal mineralization in the northern Mount Peyton intrusive suite: implications for the origin of the Mount Peyton Trend, central Newfoundland (NTS 2D/04). *In* Current Research. Government of Newfoundland and Labrador, Department of Natural Resources, Geological Survey, Report 17-1, pages 189-217.

Sandeman, H.A.I. and Honsberger, I.
2023: Gold mineralization at the Valentine Lake, Moosehead, Queensway and Kingsway projects. Geological Association of Canada, Newfoundland and Labrador Section, Fall Field Trip 2023.

Sandeman, H.A.I., Honsberger, I.W. and Camacho, A.
2022: Overview of age constraints for gold mineralization in central and western Newfoundland and new $^{40}Ar/^{39}Ar$ ages for muscovite from selected auriferous zones. Atlantic Geoscience, Volume 58.
https://doi.org/10.4138/atlgeo.2022.010

Sandeman, H.A.I., Peddle, C. and Newman, R.
2018: Beaver Brook antimony mine revisited: An update on operations and new structural and geological observations. *In* Current Research. Government of Newfoundland and Labrador, Department of Natural Resources, Geological Survey, Report 18-1, pages 123-152.

Spence-Jones, C., Jenkin, G., Boyce, A., Hill, N. and Sangster, C.
2018: Tellurium, magmatic fluids and orogenic gold: An early magmatic fluid pulse at Cononish gold deposit, Scotland. Ore Geology Reviews, Volume 102, pages 894-905.

Squires, G.C.
2005: Gold and antimony occurrences of the Exploits Subzone and Gander Zone: A review of recent discoveries and their interpretations. *In* Current Research. Government of Newfoundland and Labrador, Department of Natural Resources, Geological Survey, Report 05-1, pages 223-237.

Steele-MacInnis, M.
2018: Fluid inclusions in the system H_2O-NaCl-CO_2: An algorithm to determine composition, density and isochore. Chemical Geology, Volume 498, pages 31-44.

Strong, D.F.
1979: The Mount Peyton Batholith, central Newfoundland, a bi-modal calc-alkaline suite. Journal of Petrology, Volume 20, pages 119-138.

Sugiono, D., LaFlamme, C., Thébaud, N., Martin, L., Savard, D. and Fiorentini, M.
2022: Fault-induced gold saturation of a single auriferous fluid is a key process for orogenic gold deposit formation. Economic Geology, Volume 117, pages 1405-1414.

Tavares Nassif, M., Monecke, T., Reynolds, T.J., Kuiper, Y.D., Goldfarb, R.J., Piazolo, S. and Lowers, H.A.
2022: Formation of orogenic gold deposits by progressive movement of a fault-fracture mesh through the upper crustal brittle-ductile transition zone. Scientific Reports, Volume 12(1), page 17379.
https://doi.org/10.1038/s41598-022-22393-9

Treloar, P.J., Lawrence, D.M., Senghor, D., Boyce, A. and Harbidge, P.
2015: The Massawa gold deposit, Eastern Senegal, West Africa: An orogenic gold deposit sourced from magmatically derived fluids? *In* Ore Deposits in an Evolving Earth. *Edited by* G.R.T. Jenkin, P.A.J. Lusty, I. McDonald, M.P. Smith, A.J. Boyce and J.J. Wilkinson. Geological Society London, Special Publications, Volume 393, pages 135-160.

Tuba, G., Kontak, D.J., Choquette, B.G., Pfister, J., Hastie, E.C.G. and van Hees, E.H.P.
2021: Fluid diversity in the gold-endowed Archean orogenic systems of the Abitibi greenstone belt (Canada) I: Constraining the PTX of prolonged hydrothermal systems. Ore Geology Reviews, Volume 135, page 104221.

van den Kerkhof, A.M. and Hein, U.
2001: Fluid inclusion petrography. Lithos, Volume 55, pages 27-47.

van Staal, C. and Barr, S.M.
2012: Lithospheric architecture and tectonic evolution of the Canadian Appalachians and associated Atlantic margin. *In* Tectonic Styles in Canada: The Lithoprobe Perspective. *Edited by* J.A. Percival, F.A. Cook and R.M. Clowes. Geological Association of Canada, Special Paper 49, pages 41-95.

van Staal, C.R. and Dewey, J.F.
2023: A review and tectonic interpretation of the Taconian–Grampian tract between Newfoundland and Scotland: Diachronous accretion of an extensive fore-arc–arc–backarc system to a hyperextended Laurentian margin and subsequent subduction polarity reversal. Geological Society London, Special Publications, Volume 531(1), pages 11-46.
https://doi.org/10.1144/sp531-2022-152

van Staal, C.R., Lin, S., Valverde-Vaquero, P., Dunning, G., Burgess, J., Schofield, D. and Joyce, N.
2024: Tectonic evolution of high grade metamorphic tectonites of the Meelpaeg nappe near Port aux Basques, southwestern Newfoundland during the Silurian Salinic and early to Middle Devonian Acadian orogenies. Canadian Journal of Earth Sciences. e-First https://doi.org/10.1139/cjes-2023-0141

van Staal, C.R., Whalen, J.B., McNicoll, V.J., Pehrsson, S., Lissenberg, C.J., Zagorevski, A., van Breemen, O. and Jenner, G.A.
2007: The Notre Dame arc and the Taconic orogeny in Newfoundland. *In* 4-D Framework of Continental Crust. *Edited by* R.D. Hatcher, M.P. Carlson, J.H. McBride and J.R. Martinez Catalan. Geological Society of America Memoirs, Volume 200, pages 511-552.

Voisey, C.R., Tomkins, A. and Xing, Y.
2020a: Analysis of a telescoped orogenic gold system: Insights from the Fosterville Deposit. Economic Geology, Volume 115, pages 1645-1664.
https://doi.org/10.5382/econgeo.4767

Voisey, C.R., Willis, D. Tomkins, A.G., Wilson, C.J.L., Micklethwaite, S., Salvemini, F., Bougoure, J. and Rickard, W.D.A.
2020b: Aseismic refinement of orogenic gold systems. Economic Geology, Volume 115(1), pages 33-50.
https://doi.org/10.5382/econgeo.4692

Waldron, J.W.F., Barr, S.M., Park, A.F., White, C.E. and Hibbard, J.P.
2015: Late Paleozoic strike-slip faults in Maritime Canada and their role in the reconfiguration of the northern Appalachian orogen. Tectonics, Volume 34, pages 1661-1684.

Waldron, J.W.F., McNicoll, V.J. and van Staal, C.R.
2012: Laurentia-derived detritus in the Badger Group of central Newfoundland: deposition during closing of the Iapetus Ocean: Canadian Journal of Earth Sciences, Volume 49, no. 1, pages 207-221.
https://doi.org/10.1139/e11-030

Waldron, J.W.F. and van Staal, C.R.
2001: Taconian orogeny and the accretion of the Dashwoods block: a peri-Laurentian microcontinent in the Iapetus Ocean. Geology, Volume 29, pages 811-814.

Wang, C., Wang, T., Staal, C., Hou, Z. and Lin, S.
2024: Evolution of Silurian to Devonian magmatism associated with the Acadian orogenic cycle in eastern and southern Newfoundland Appalachians: Evidence

for a three-stage evolution characterized by episodic hinterland- and foreland-directed migration of granitoid magmatism. Geological Society of America Bulletin, Volume 136, pages 4648-4670. https://doi.org/10.1130/B37336.1

Ward, J., Mavrogenes, J., Murray, A. and Holden, P.
2017: Trace element and sulfur isotopic evidence for redox changes during formation of the Wallaby gold deposit, Western Australia. Ore Geology Reviews, Volume 82, pages 31-48.

Whalen, J.B., Jenner, G.A., Longstaffe, F.J., Gariepy, C. and Fryer, B.
1997: Implications of granitoid geochemical and isotopic (Nd, O, Pb) data from the Cambro–Ordovician Notre Dame arc for the evolution of the Central Mobile Belt, Newfoundland Appalachians. *In* The Nature of Magmatism in the Appalachian Orogen. *Edited by* A.K. Sinha, J.B. Whalen and J.P. Hogan. Geological Society of America Memoir, Volume 191, pages 367-395.

Whalen, J.B., McNicoll, V.J., van Staal, C.R., Lissenberg, C.J., Longstaffe, F.J., Jenner, G.A. and van Breemen, O.
2006: Spatial, temporal and geochemical characteristics of Silurian collision zone magmatism, Newfoundland Appalachians: An example of a rapidly evolving magmatic system related to slab break-off. Lithos, Volume 89, pages 377-404. https://doi.org/10.1016/j.lithos.2005.12.011

Whitney, D.L. and Evans, B.W.
2010: Abbreviations for names of rock-forming minerals. American Mineralogist, Volume 95, pages 185-187.

Wilkinson, J.J.
2001: Fluid inclusions in hydrothermal ore deposits. Lithos, Volume 55, pages 229-272.

Williams, H.
1979: Appalachian Orogen in Canada. Canadian Journal of Earth Sciences, Volume 16, pages 792-807. https://doi.org/10.1139/e79-070

Williams, H., Colman-Sadd, S.P. and Swinden, H.S.
1988: Tectonic-stratigraphic subdivisions of central Newfoundland. *In* Current Research, Part B. Eastern and Atlantic Canada, Geological Survey of Canada, Paper 88-1B, pages 91-98.

Williams, H. and St. Julien, P.
1982: The Baie Verte-Brompton Line: Early Palaeozoic continent ocean interface in the Canadian Appalachians. *In* Major Structural Zones and Faults of the Northern Appalachians. *Edited by* P. St-Julien and J. Beland. Geological Association of Canada, Special Paper 24, pages 177-208.

Williams, S.H.
1989: New graptolite discoveries from the Ordovician of central Newfoundland. *In* Current Research. Government of Newfoundland and Labrador, Department of Mines, Geological Survey, Report 89-1, pages 149-157.

1993: More Ordovician and Silurian graptolites from the Exploits Subzone. *In* Current Research. Government of Newfoundland and Labrador, Department of Mines and Energy, Geological Survey Branch, Report 93-1, pages 311-315.

Williams-Jones, A.E., Bowell, R.J. and Migdisov, A.A.
2009: Gold in solution. Elements, Volume 5(5), pages 281-287.

Willner, A.P., van Staal, C.R., Zagorevski, A., Glodny, J., Romere, R.L. and Sudo, M.
2018: Tectonometamorphic evolution along the Iapetus suture zone in Newfoundland: Evidence for polyphase Salinic, Acadian and Neoacadian very low- to medium-grade metamorphism and deformation. Tectonophysics, Volumes 742–743, pages 137-167. https://doi.org/10.1016/j.tecto.2018.05.023

Wilton, D.H.C. and Strong, D.F.
1986: Granite-related gold mineralization in the Cape Ray Fault Zone of southwestern Newfoundland. Economic Geology. Volume 81, pages 281-295.

Yardley, B.W.D.
2005: 100th Anniversary Special Paper: Metal Concentrations in Crustal Fluids and Their Relationship to Ore Formation. Economic Geology, Volume 100(4), pages 613-632.

Yardley, B.W.D. and Cleverley, J.S.
2015: The role of metamorphic fluids in the formation of ore deposits. Geological Society of London, Special Publications 393(1), pages 117-134.

Zhong R., Brugger J., Tomkins A.G., Chen Y. and Li W.
2015: Fate of gold and base metals during metamorphic devolatilization of a pelite. Geochimica et Cosmochimica Acta, Volume 171, pages 338-352.

Zoheir, B., Steele-MacInnis, M. and Garbe-Schönberg, D.
2019: Orogenic gold formation in an evolving, decompressing hydrothermal system: Genesis of the Samut gold deposit, Eastern Desert, Egypt. Ore Geology Reviews, Volume 105, pages 236-257.